1958-07

Correlation measurements in the boundary layer of a flat plate

Martin, William L.

Massachusetts Institute of Technology

CORRELATION MEASUREMENTS IN THE BOUNDARY LAYER OF A FLAT PLATE

WILLIAM L. MARTIN III
AND
ARTHUR T. WHITE

CORRELATION MEASUREMENTS IN THE BOUNDARY LAYER OF A FLAT PLATE

by

William L. Martin III
Lieutenant, U.S. Navy
Nav. E., Massachusetts Institute of Technology (1954)

Arthur T. White
Lieutenant Commander, U. S. Navy
B.S., Massachusetts Institute of Technology (1948)

Submitted in Partial Fulfillment
of the Requirements for the
Degree of Master of Science

at the

MASSACHUSETTS INSTITUTE OF TECHNOLOGY

July, 1958

Cambridge, Massachusetts
July 21, 1958

Professor Leicester F. Hamilton
Secretary of the Faculty
Massachusetts Institute of Technology
Cambridge 39, Massachusetts

Dear Sir:

In accordance with the requirements of the degree of Master of Science, we herewith submit a thesis entitled "Correlation Measurements in the Boundary Layer of a Flat Plate."

ABSTRACT

CORRELATION MEASUREMENTS IN THE

BOUNDARY LAYER OF A FLAT PLATE

by

WILLIAM L. MARTIN, III, LIEUTENANT, U. S. NAVY

ARTHUR T. WHITE, LIEUTENANT COMMANDER, U. S. NAVY

Submitted to the Department of Nuclear Engineering on July 21, 1958, in partial fulfillment of the requirements for the degree of Master of Science.

The objective of this thesis was to assemble an instrumentation system and make limited measurements of correlation quantities in the boundary layer of a flat plate with an unheated starting length.

A system consisting of suitable probes, amplifier, calibration and measuring circuits, and voltmeter was assembled and tested. A series of measurements of the characteristic quantities of turbulent fluid flow were made by a traverse through the boundary layer at one location on the plate.

Although there is considerable scatter in the results, the system can be expected to give satisfactory results after the recommended equipment modifications and test procedures are effected.

Thesis Supervisor: R. J. Nickerson
Title: Assistant Professor of Mechanical Engineering

TABLE OF CONTENTS

Table of Contents

LIST OF FIGURES

List of Figures

I. INTRODUCTION

In the theory of turbulent fluid flow and heat transfer, the correlated quantities $\overline{uv}$ and $\overline{vt}$ have particular significance. The simplified equations that describe the boundary layer over a heated flat plate may be written as: (See Appendix B for derivation)

Momentum transfer:

$$\frac{\partial}{\partial x}\left(\bar{P} + \rho \bar{U}^2 + \rho \overline{u^2} \right) = \frac{\partial}{\partial y}\left(\mu \frac{\partial \bar{U}}{\partial y} - \rho \bar{U}\bar{V} - \rho \overline{uv} \right); \qquad (1)$$

Energy transfer:

$$\frac{\partial}{\partial x}\left(\bar{U}\bar{T} + \overline{ut} \right) = \frac{\partial}{\partial y}\left(\mathfrak{L} \frac{\partial \bar{T}}{\partial y} - \bar{V}\bar{T} - \overline{vt} \right). \qquad (2)$$

Analytical solution of these equations is possible only under very restrictive conditions. For such solutions the following definitions of the eddy shear stress coefficient, $\mathfrak{E}_m$ and the eddy energy transfer coefficient, $\mathfrak{E}_h$ are introduced:

$$\overline{uv} = -\mathfrak{E}_m \frac{\partial \bar{U}}{\partial y} \qquad (3)$$

and

$$\overline{vt} = -\mathfrak{E}_h \frac{\partial \bar{T}}{\partial y} \qquad (4)$$

Assumed analogies between these coefficients together with suitable boundary conditions has been an accepted method for solving problems for a great many years. Very little work has been done, however, to actually measure $\overline{uv}$ and $\overline{vt}$ and experimentally substantiate the theory.

The literature contains little data other than that of Johnson in ref. 1. He obtained measurements of these and other quantities in the

I. INTRODUCTION

In the theory of two-dimensional fluid flow and heat transfer, the interrelated quantities $\overline{uv}$ and $\overline{uT}$ have particularly significance. The simplified expressions that describe the boundary layer over a heated flat plate may be written as

(See Appendix I for derivation)

Momentum transfer:

$$\frac{\partial}{\partial x}(u^2 + \epsilon_M \frac{\partial u}{\partial y}) = \frac{\partial^2 u}{\partial y^2} - \frac{1}{\rho}\frac{dP}{dx} - \frac{\partial \overline{uv}}{\partial y} \qquad (1)$$

Energy transfer:

$$\frac{\partial u}{\partial x}(uT + \epsilon_H \frac{\partial T}{\partial y}) = \frac{\partial^2 T}{\partial y^2} - \frac{\partial \overline{uT}}{\partial y}. \qquad (2)$$

Analytical solution of these equations is possible only under very restrictive conditions. For most problems the following definitions of the eddy shear stress coefficient, ϵ_M and the eddy energy transfer coefficient, ϵ_H are introduced:

$$\overline{uv} = -\epsilon_M \frac{\partial u}{\partial y} \qquad (3)$$

and

$$\overline{uT} = -\epsilon_H \frac{\partial T}{\partial y} \qquad (4)$$

Various analogies between these coefficients together with suitable boundary conditions have been developed which for solving problems for a great many cases. They little help here, however, to actually measure $\overline{uv}$ and $\overline{uT}$ and experimentally substantiate the theory.

The literature contains little more than hint of values in col. 1. No detailed measurements of these and other quantities in the

boundary layer over a flat plate with an unheated starting length. His results are given for only one vertical exploration of the boundary layer, and they agree with the expected behavior of $\overline{uv}$ and $\overline{vt}$ as functions of distance from the heated plate.

It has been proposed that a thorough investigation of the thermal boundary layer properties be undertaken at M.I.T. Therefore, it is of fundamental importance to design an instrumentation system of sufficient sensitivity and accuracy to evaluate such properties.

It was the purpose of this thesis to assemble such an instrumentation system and make preliminary measurements over a heated flat plate. Theoretically a hot-wire anemometer system will provide sufficient data for calculating $\overline{uv}$ and $\overline{vt}$. A basic system was assembled and tested. Certain components were available in the laboratory, and the remaining items were selected from commercially available instruments. Appendix D contains a description of the equipment.

II. PROCEDURES

The experiment was conducted in the Heat Measurement Laboratory using one of the small scale wind tunnels. The boundary layer was developed over a 40" aluminum plate resting on the bottom of the tunnel. The last twelve-inch section of the plate was heated by a coil of resistance heating wire on the underside. Measurements were made along a vertical traverse through the boundary layer ten inches from the start of the heated section.

The hot-wire anemometer equipment consisted of hot-wire probes, a Flow Corporation HWB amplifier and bridge unit and a Ballantine 320 true root-mean-square volt-meter.

Two different hot-wire anemometer probes were used. One was a single-wire; the other a V-wire probe. Appendix D describes the equipment in greater detail.

Because the V-probe soon proved unacceptable, the single-wire probe was used thereafter. Orienting the wire first at plus 45°, then at minus 45° to the free stream velocity gave the desired data. Since only the time-averaged quantities enter the calculations, data for each orientation did not need to be taken at the same time.

After thermal aging for a half-hour, the wire was carefully calibrated by recording the wire current at each resistance ratio for various wind velocities. A micromanometer was used to obtain accurate velocities.

A plot of I^2 vs $\sqrt{U}$ appears in Fig. 8 for γ = 1.2 and 1.4. These

II. [illegible]

The experiment was conducted in the Mare Imbrium Laboratory using one of the small scale wind tunnels. The boundary layer was developed over a 60' aluminum plate resting on the bottom of the tunnel. The test section-inlet section of the plate was heated by a coil of resistance heating wire on the underside. Thermocouples were then along a vertical traverse through the boundary layer and lying from the start of the heated section.

The hot-wire anemometer employed consisted of two-wire probes, a flow compensation box amplifier and bridge unit and a Hallamotion 380 true rms-zero-suppress volt-meter.

Two different hot-wire anemometer probes were used. One was a single-wire, the other a V-wire probe. Appendix B describes the equipment in greater detail.

Because the V-probe uses crossed anemometers, the single-wire probe was used therefore. Obtaining the wire first or plus $\overline{uv}$, then an minus $\overline{uv}$ to the flow stream velocity gave the desired data. Those only the time-averaged quantities enter the calculations, data for each orientation did not need to be taken at the same time.

After thermal aging for a half-hour, the wire was carefully calibrated by recording the wire output at each temperature until the various wind velocities. A micromanometer was used to obtain accurate velocities,

a plot of E_w^2 vs $\overline{V}^2$ appears in fig. 6 for γ = 1.3 was i.d. These

curves agree with the characteristic straight lines predicted by the King equation.

From these curves it is possible to calculate I' from equation (36), where

$$I' = \frac{C_2}{4I\sqrt{U}} \quad . \tag{5}$$

As equation (72) predicts, the quantities $\overline{uv}$ and $\overline{vt}$ are related by

$$\frac{1}{2}\left(\frac{i_s}{I'}\right)^2 \left[\left(\frac{M_{sn}^2 - M_n^2}{M_{scn}^2 - M_{sn}^2}\right)_b - \left(\frac{M_{sn}^2 - M_n^2}{M_{scn}^2 - M_{sn}^2}\right)_a\right] = -\overline{uv} + \left\{\frac{\sqrt{2}}{4I'} \frac{\alpha e}{\gamma - [1 + \alpha_e(\bar{T}_g - \bar{T}_e)]}\right\} (I_a + I_b)\,\overline{vt}, \tag{6}$$

where the subscripts a and b denote the quantities for the two wire orientations. It is important that the wires of whatever probe is used be correctly angled to the flow, i.e. $\pm 45^\circ$ for this case.

The procedure for measuring and calculating these quantities follows:

Ref. 12, the HWB Instruction Book, describes how to compute the square-wave current and how to set the desired resistance ratios. Briefly, the "Bridge Null" dial of the HWB is adjusted to balance the bridge for a "cold" current in the wire of about one and a half milliamps.

At one of the available resistance ratios, the current is increased in the wire until the bridge is again balanced. The values of resistance ratio and "bridge null" dial setting then enter the calculation of square-wave current as shown in Appendix E.

The following sequence of readings was obtained at the maximum tunnel velocity of 26 ft/sec with the plate first unheated, then heated:

curves agree with the characteristic straight lines predicted by the King equation.

From these curves it is possible to calculate $\bar{i}$ from equation (36), where

$$\bar{i} = \frac{\quad}{\quad} \qquad (3)$$

As equation (12) predicts, the quantities $\overline{ev}$ and $\overline{vt}$ are related by

$$\frac{1}{2}\left(\frac{I_1}{C_m}\right)^2 \left[\left(\frac{\quad}{\quad}\right) - \left(\frac{\quad}{\quad}\right)^2\right]^{-1} \left[\left(\frac{\quad}{\quad}\right) - \left(\frac{\quad}{\quad}\right)\right] = \left\{\frac{\quad}{\quad} - \left[1 + e^{\alpha(\beta - \quad)}\right]\right\} (\lambda^a + \lambda^b)\ \overline{vt}^2 \qquad (5)$$

where the subscripts a and b denote the quantities for the two wire orientations. It is important that the wires of whatever probe is used be correctly angled to the flow, i.e. $\pm 45^\circ$ for this case.

The procedure for measuring and calculating these quantities follows: Ref. 12, the DCA Instruction Book, describes how to compute the square-wave current and how to set the desired resistance ratios. Briefly, the "Bridge Null" dial of the DCA is adjusted to balance the bridge for a "cold" current in the wire of about one and a half milliamps.

At one of the available resistance ratios, the current is increased in the wire until the bridge is again balanced. The values of resistance ratio and "Bridge Null" dial setting then enter the calculation of square-wave current as shown in Appendix B.

The following sequence of readings was obtained at the maximum tunnel velocity of 16 ft/sec with the plate first unheated, then heated:

With the wire at plus 45°, values of M_{sn}, M_{scn} and I_a were recorded at resistance ratios of 1.2 and 1.4. This was repeated at predetermined distances, y, above the plate as measured by the micro-traverse gear, starting where the probe shank touched the plate.

Values of M_{sn}, M_{scn} and I_b were subsequently recorded with the wire at minus 45° for the same values of y.

The purpose of the hot and cold plate readings becomes clear when one assumes t = 0 for the unheated plate. Then equation (72) is

$$\overline{uv} = -\frac{1}{2}\left(\frac{i_s}{I'}\right)^2 \left[\left(\frac{M_{sn}^2 - M_n^2}{M_{scn}^2 - M_{sn}^2}\right)_b - \left(\frac{M_{sn}^2 - M_n^2}{M_{scn}^2 - M_{sn}^2}\right)_a\right]. \qquad (7)$$

However, with the heated plate the full equation applies.

The remaining part of the coefficient of $\overline{vt}$, $\dfrac{\alpha_e}{\gamma - [1 + \alpha_e(T_g - T_e)]}$, may be calculated as shown in Appendix E.

Making measurements at two resistance ratios gives two simultaneous equations at each y. Solution of these equations gives $\overline{uv}$ and $\overline{vt}$ for the hot plate, and $\overline{uv}$ for the cold plate. With the plate cold $\overline{uv}$ is over-determined, so the average of the two equations was taken.

A traverse of the boundary layer with the wire perpendicular to the mean flow gives a comparison of the wire current with that in the free stream. From the I^2 vs $\sqrt{U}$ calibration data on the wire, the average velocity as a function of y can be picked off.

Similarly, a measurement of wire currents at a position first with the plate heated, then unheated, allows calculation of the temperature rise above ambient by the method of Appendix E.

III. RESULTS

A. Figure 1 shows $\overline{uv}/U_\infty^2$ as a function of vertical distance from the plate for the heated and unheated conditions. Reasonable agreement with published data is demonstrated. The value of this quantity is greater in the heated plate condition than for the cold plate, as was noted in reference (1).

Figure 2 is a graph of the temperature $(\bar{T}g-Te)/(Ts-Te)$ and velocity $(\bar{U}/U_\infty)$ profiles across the boundary layer.

Figure 3 is a plot of $\overline{uv}/U_\infty^2$ and $\overline{vt}/U_\infty\,(Ts-Te)$ for the heated plate. The best data obtained is shown. The extreme scatter of the data precludes computing εm and εh as functions of y in order to establish an analogy between them.

B. The basic instrumentation selected includes: (a) a hot wire probe with 0.00015" tungsten wires; (b) a Flow Corporation, Hot Wire Anemometer, model HWB; and (c) a modified Ballantine Laboratory, True RMS Voltmeter, model 320. This equipment will measure accurately the properties of a momentum boundary layer. It is probable that the additional properties of a thermal boundary layer can also be detected with this instrumentation; however, this cannot be stated conclusively. Appropriate recommendations are included in section VI. The equipment is illustrated in figure 4.

III. [illegible]

4. Figure 3 shows $\overline{u}/\overline{u}_\infty$ as a function of vertical distance from the plate for the blocked and unblocked conditions. Reasonable agreement with published data is demonstrated. The value of this quantity is greater in the heated flow conditions than for the cold plate, as noted in reference (1).

Figure 4 is a graph of the temperature $(\overline{T}-T_\infty)/(T_w-T_\infty)$ and velocity $(\overline{u}/\overline{u}_\infty)$ profiles across the boundary layer.

Figure 5 is a plot of $\overline{u}/\overline{u}_\infty$ and $\overline{v}/\overline{u}_\infty$ (T_w-T_∞) for the heated plate. The heat data obtained is shown. The universe quality of the data precludes comparing Eq. (2) or (3) as functions of y in order to establish an analogy between them.

5. The basic instrumentation utilized includes: (a) a hot wire probe with a digital temperature system; (b) a flow conditioning, hot wire anemometer, model 1053; and (c) a multiple Baldwin Lapcrimary, Time Base Voltmeter, model 139. This equipment will accurately investigate the properties of a convection boundary layer. It is probable that the additional properties of a thermal boundary layer can also be measured with this instrumentation; however, data cannot be stated categorically. Appropriate recommendations are included in Section VI. The system is illustrated in Figure 4.

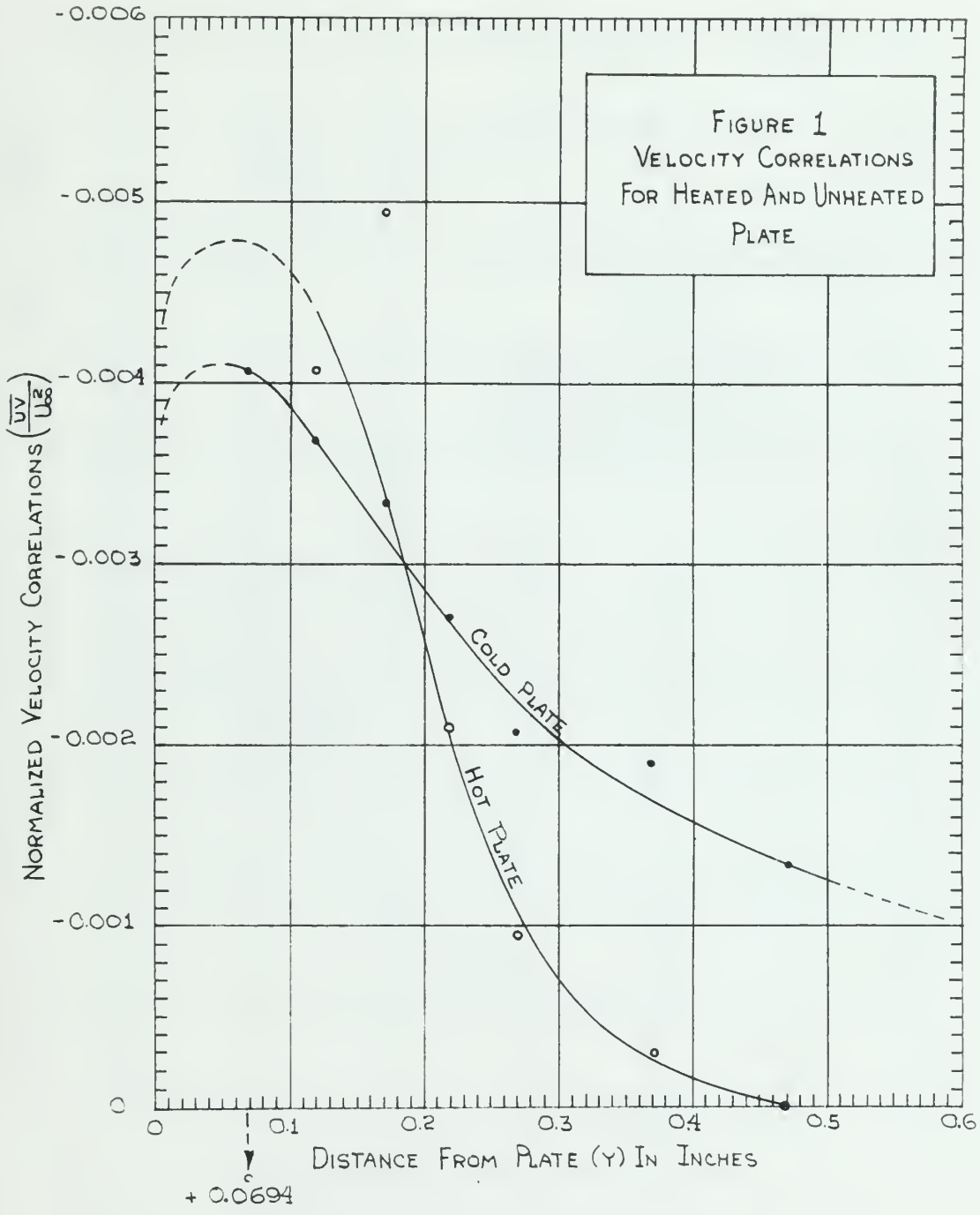
FIGURE 1
VELOCITY CORRELATIONS
FOR HEATED AND UNHEATED
PLATE
NORMALIZED VELOCITY CORRELATIONS $\left(\frac{\overline{uv}}{U_\infty^2}\right)$
-0.006
-0.005
-0.004
-0.003
-0.002
-0.001
0
0
0.1
0.2
0.3
0.4
0.5
0.6
COLD PLATE
HOT PLATE
DISTANCE FROM PLATE (Y) IN INCHES
c
+ 0.0694

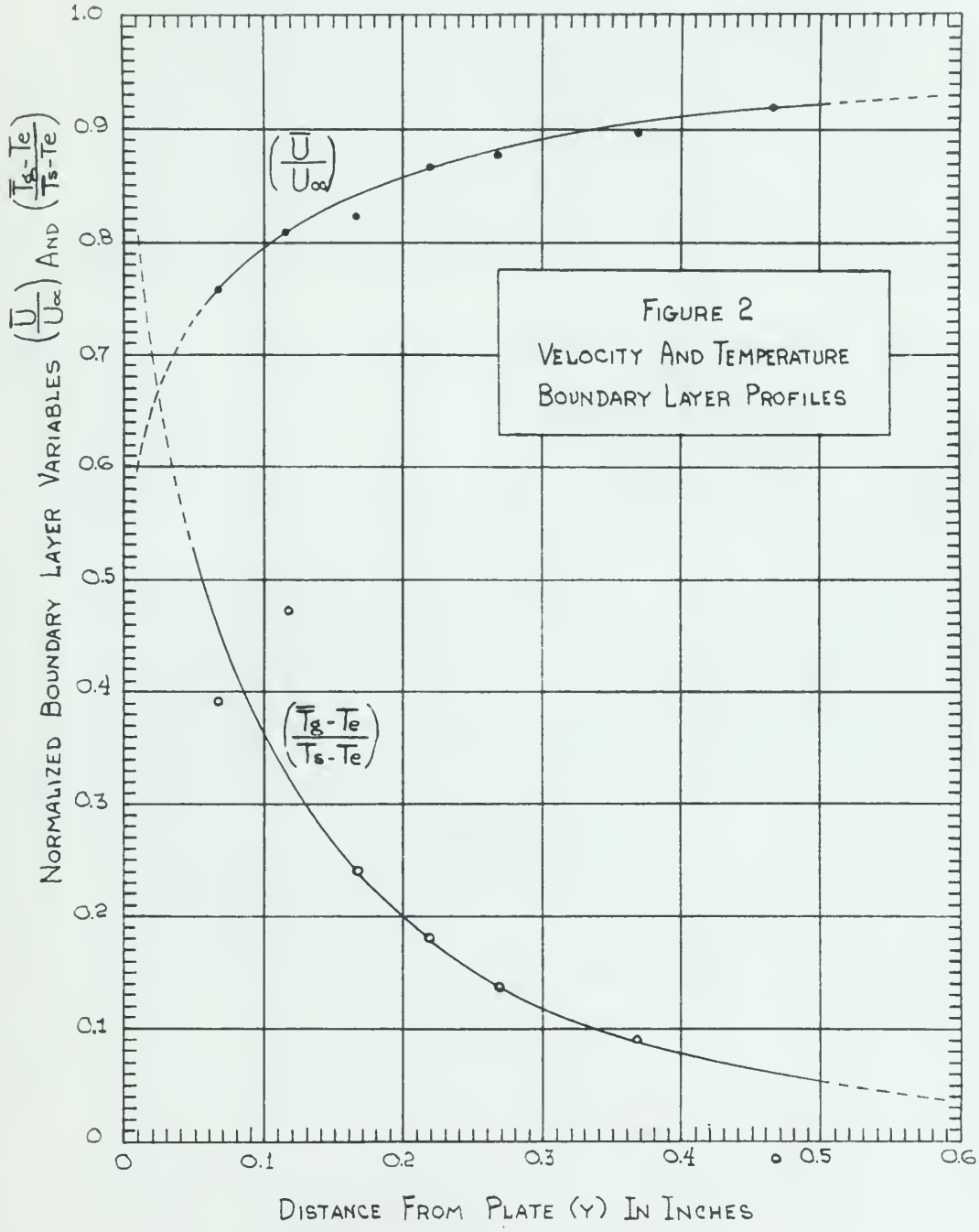

Figure 2
Velocity And Temperature
Boundary Layer Profiles

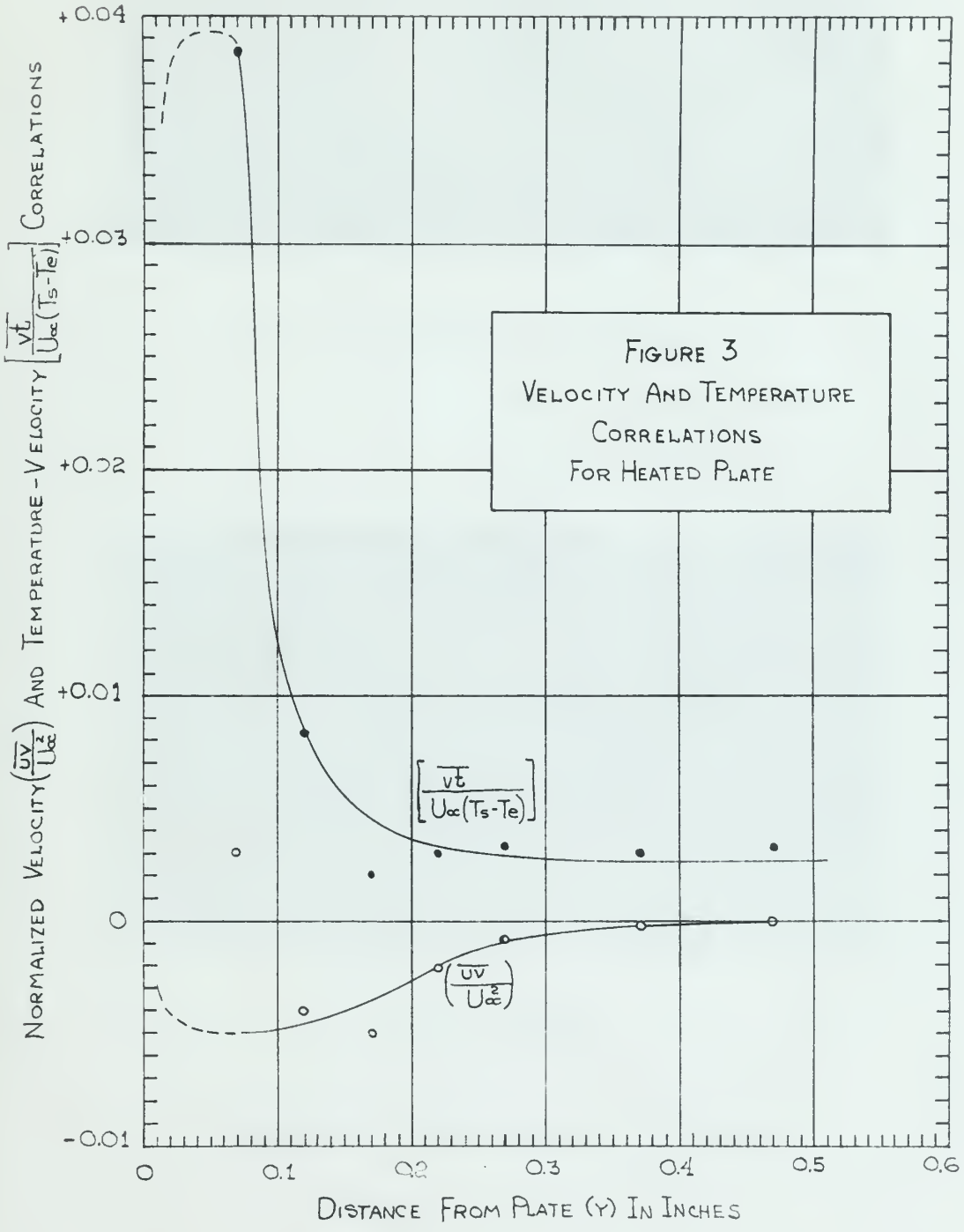

Figure 3
Velocity And Temperature
Correlations
For Heated Plate

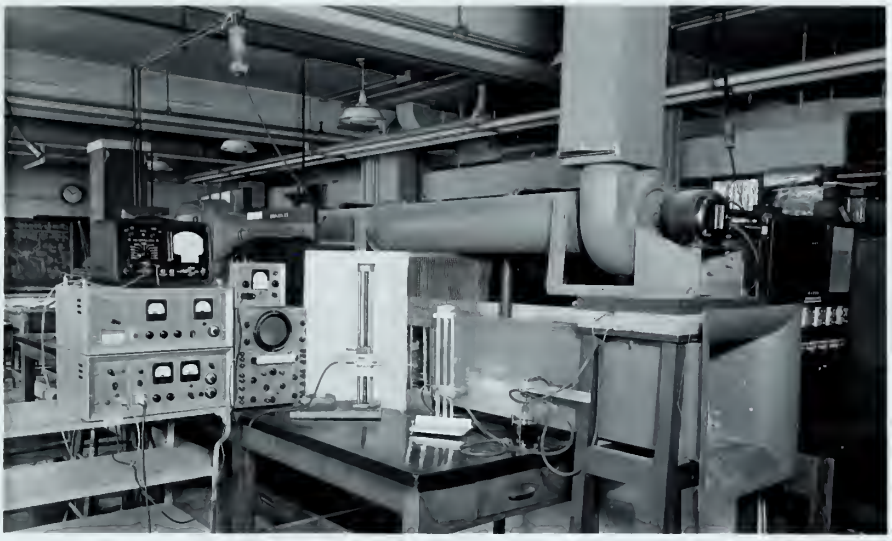

(a). Equipment Arrangement

(b). Probes

Figure 4 - Experimental Equipment

IV. DISCUSSION OF RESULTS

A. The plot of $\overline{uv}/U_\infty^2$ in Fig. 1 has about the same order of magnitude, although somewhat higher, as that shown by Johnson in ref. 1. The slope of this curve is much greater than Johnson's however. He did obtain two or three points close to the heated plate that are much higher than those for the cold plate. Further from the plate Johnson's velocity correlation quantities are almost identical for the heated and unheated conditions.

On the other hand, the quantities shown in Fig. 1 for the heated plate remain generally higher than for the cold plate over the span measured. This difference could easily be due to experimental error, however there is a possible explanation. Thermal convection from the heated plate could be expected to disrupt the laminar sublayer causing some increase in the turbulence of the flow close to the plate. Fluid moving from the sublayer would have lower velocities and therefore tend to correlate a(-u) with a(-v) to add to the quantity $(-\overline{uv})$ for the cold plate.

B. The plots of $\overline{U}/U_\infty$ and (Tg-Te)/(Ts-Te) as a function of distance from the plate show the typical characteristics of these functions. The velocity profile indicates that measurements should be taken closer to the plate to further delineate the shape of the curve. To do this a much shorter hot-wire would be needed.

IV. DISCUSSION OF RESULTS

8. The plots of $\overline{uv}/U_\infty^2$ in Fig. 3 have the same order of magnitude, although somewhat higher, as that shown by Johnson in ref. 1. The slope of this curve is much greater than Johnson's however. He did obtain two or three points close to the heated plate that are much higher than those for the cold plate. Further tests in Johnson's velocity correlation quantities are almost identical for the heated and unheated conditions.

On the other hand, the quantities shown in Fig. 4 for the heated plate remain generally higher than for the cold plate over the span measured. This difference could easily be due to experimental error, however there is a possible explanation. Thermal convection from the heated plate could be expected to disrupt the laminar sublayer causing some increase in the fluctuations of flow close to the plate. Fluid moving from the subplate would have lower velocities and therefore tend to correlate $u(-v)$ with $u(-v)$ to add to the quantity $(-\overline{uv})$ for the cold plate.

9. The plots of $\overline{u^2}/U_\infty^2$ and $(T_g-T_e)/(T_e-T_s)$ as a function of distance from the plate show the typical characteristics of these functions. The velocity profile indicates that measurements should be taken closer to the plate to further delineate the shape of the curve. To do this a much shorter hot-wire would be needed.

Extrapolating the curve of Tg-Te in Fig. 10 to the plate gave an estimated plate surface temperature, Ts, of 8° C above ambient. Such a low temperature difference made temperature measurements difficult.

Another more accurate method of measuring temperature would be to record the bridge null at "cold current" (about one and a half milliamps) while traversing the boundary layer. For this a bridge galvanometer amplifier is required to enable more accurate bridge null settings than is possible with this model HWB. The later HWP models do incorporate such an amplifier.

C. As stated in the Results, the scatter in the computed points $\overline{vt}/U_\infty$ (Ts-Te) in Fig. 3 did not warrant calculation of Em and Eh by equations (3) and (4). This is one of the most important ultimate goals of these measurements that was not realized in this thesis. No reliable curve of $\overline{vt}$ can be inferred, and several attempts to deduce better values of this quantity produced no better results than those shown. A higher plate temperature would likely give larger, more-easily-measured quantities.

The data does not show the predicted behavior of $\overline{uv}$ and $\overline{vt}$ going to zero at the plate. At the closest approach, the center of the wire is still 0.068 inches from the plate. Any decrease in these quantities must therefore be inside this distance.

D. The equations (69) and (70) in Appendix B for two wires apply also for wires mounted on an X-probe. Johnson used an X-probe with both wires hot for detecting velocity fluctuations and a single cold wire close by for temperature variations. The hot-wire theory predicts that it is unnecessary to use more than one hot-wire. Since equation (71) has five unknowns, it is necessary only to make measurements with one wire at five resistance ratios and solve the resulting equations simultaneously.

If two wires on an X-probe are controlled independently by two HWB's with outputs measured on separate meters, equations (69) and (70) may be solved together at five resistance ratios to yield the boundary layer properties. The two important correlated quantities are dominant in equation (72).

The practice in this experiment of orienting the probe at $\pm 45^{\circ}$ simulated an X-probe and eliminated the problem of matching the two wires to close tolerances. Experience with the V-probe supports the comment made by Johnson (p. 54 of ref. 1) that it is unlikely I', I, α_e, the time constant, length, diameter and other characteristics of two wires can ever be matched simultaneously.

A few comments on the V-probe may warn others of the pitfalls of its peculiarities.

It was first discovered that the resistance of the common current lead and center needle is unavoidably in one arm of the bridge circuit. Since the voltage across the center lead is proportional to the sum of the two wire currents, the bridge null for one wire is affected by current in the other.

The second problem is serious, particularly in a thin boundary layer. The two wires are sufficiently separated to be in different stream conditions and do not correlate quantities at a point.

The third problem has been discussed - that of matching any two wires.

Finally, several times it was noted that wires on the V-probe were not taut and straight several hours after rewiring. This means that wires are not at the specified angle to the stream.

E. One problem that detracts from the accuracy of the results is ambient temperature variations while the measurements are being made in a traverse

through the boundary layer. Using the minimum number of two resistance ratios at each y, it required four to six hours to take data at seven points. Since the ambient temperature can change by several degrees during this time, it is desirable to have a constant-temperature air input to the tunnel.

It was noticed that there was considerable velocity fluctuation in the free stream on the axis of the tunnel. This masked the "edge" of the momentum boundary layer.

To reduce the above defects of this tunnel it is desirable that the entrance be fitted with a plenum where the air can be heated a few degrees above the ambient at the same time the velocity fluctuations are being smoothed.

Along with tunnel entrance modifications other test facility improvements should be incorporated.

Although a complete survey of the boundary layer should include measurements at various distances along the plate, it would be well for the uninitiated to practice in boundary layers at least two inches thick. This means having an unheated starting length of at least 40 inches long and a heated section 30 inches long. The tunnel should be three to four feet wide to approximate an infinitely wide plate.

The heated plate should be well-insulated on the bottom and equipped with heating coils and thermocouples for obtaining a constant (q/A) or constant temperature plate as desired.

F. Of all the problems encountered in this experiment, that of measuring accurate (i.e. less than 5%) true root-mean-square voltages caused the most consternation. The best available information indicated that the Ballantine Model 320 and Flow Corporation TBM were the only two meters commercially available reputed to measure RMS voltages on a random signal.

When the short time constant of the Model 320 was lengthened, it became the most reliable instrument. However, both meters exhibited the annoying characteristic of indicating different values of the same voltage on adjacent scales. The TBM became unusable for this reason, and the Model 320 gave ambiguous readings only at times. The limited "crest factor" of the Model 320 could permit peak clipping of the signal on the lower scale and thereby alter the waveform. However, such should not be the case for the TBM with its much higher "peak factor."

This problem was not resolved and is the most likely cause of the wide scatter in the calculated results. Knowing that this problem existed provided the hint to smooth the data as a function of y before re-calculating $\overline{uv}$ and $\overline{vt}$. Even so the improvement was not marked.

It is interesting to note that the literature reviewed for this thesis makes no mention of true RMS measurements or time-averaged readings in similar work.

The Model 320 could be improved by making a well-designed permanent modification to obtain a long time constant, mean square averaging circuit. If the meter time constant cannot be suitably controlled, then a five to ten minute time recording of the output could be graphically integrated to establish the best value of each voltage.

A more elaborate scheme of calibrating the meter is needed. The most appropriate method would be to use a variable-frequency generator with a calibrated output adjustable from one millivolt to one volt. It could be used to resolve the problem of peak clipping of the signals.

G. One test of accurate data is its repeatability. Time permitted little experimenting along this line, but it was often noted that the bridge could be rebalanced and currents reset to a maximum variation of one part in 150 or 0.7%.

In the presence of signal fluctuations the galvanometer fluctuated also. This was particularly noticeable at high resistance ratios. In setting average currents it became necessary to average the needle fluctuations by eye. Occasionally this led to variations of one part in 75 or 1.3%. Provision of a selectable time constant on the galvanometer would assist in setting more accurate currents and resistance ratios.

At the time they were taken, meter readings could be averaged within 2% in spite of the slow fluctuations. However, it was rarely possible to repeat the data at a point because ambient conditions had changed. On the few occasions when it was possible to check results, meter readings were well within 5% barring anomalies already discussed.

V. CONCLUSIONS

Hot wire anemometer theory predicts that both of the desired correlation quantities, $\overline{uv}$ and $\overline{vt}$, can be obtained with a single, matched, X-wire probe. Due to the extremely small volume affected by the fluctuation quantities at any instant, velocity-temperature sensing elements in a single probe is preferable to separate probe sensing elements.

The instrumentation system, modified as recommended in section VI, should yield data of sufficient accuracy for calculation of all the thermal boundary layer properties. The results presented do not affirm this statement without question, but they do indicate that further careful investigation is warranted. Refinement of instrument sensitivity and experimental technique are the paramount requisites.

VI. RECOMMENDATIONS

The following modifications of instrumentation and facilities are required for accurate measurements of the thermal boundary layer properties:

(1) Permanent modification of the meter circuit of a Ballantine 320 to obtain a long time constant averaging period;

(2) Accurate calibration of all the range scales on the voltmeter by use of an accepted standard frequency meter which has a calibrated voltage output;

(3) Construction of an X-wire probe with the wires oriented accurately at 90° to each other and their resistance matched with 2%;

(4) Construction of a longer heated section for the plate to increase the boundary layer thickness;

(5) Construction of a larger scale wind tunnel with an inlet heated plenum chamber to insure a constant temperature, constant velocity air stream in the tunnel;

(6) Procurement of an additional HWB, modified to include a sum and difference unit in lieu of the amplifier section.

In addition, the data processing techniques should be refined as follows:

(7) An averaging technique must be used over and above that which is provided in (1) above - e.g., averaging of sequentially timed observations, or graphical integration of the recorded output of the voltmeter;

(8) All five resistance ratios permitted by the wire size must be used

VI. CONCLUSIONS

The following modifications of instrumentation and facilities are required for successful measurements of the thermal boundary layer properties:

(1) Pressure modification at the outer stream of a bellmouth is to provide a long flow constant Reynolds number;

(2) Accurate calibration of all the flow meters as the maximum is one of an accepted standard frequency meter which has a calibrated working output;

(3) Construction of an S-duct tube with the three sections normally at 90° to each other and under pressure relief with Mg;

(4) Construction of a longer inviscid section for the tube to increase the boundary layer thickness;

(5) Construction of a larger scale wind tunnel with an inlet honeycomb screen chamber to insure a uniform temperature, pressure velocity air stream in the tunnel;

(6) Procurement of an additional DVM, available to include a one mV difference scale in lieu of the negligible reading.

In addition, the above proposed modifications should be helpful in further:

(7) In computing turbulence must be used when such shown in provided in (1) above - e.g., computing of temperature, or graphical integration of the recovery region of the boundary;

(8) All flow restrictions problem permitted by the wire size must be used

to calculate all five terms of equation #7/ until their order of magnitude is firmly established. Programming of these equations for computer use would considerably speed data analysis.

APPENDIX A

NOMENCLATURE

A	Cross-sectional area.
c	Heat capacity of wire.
C_p	Heat capacity of fluid at constant pressure.
C_1, C_2	Constants.
D	Wire diameter.
D^*	Wire diameter, units of 0.001 inch.
e	Voltage (general).
e_c	Output voltage from the amplifier due to square-wave current alone imposed on the wire.
e_{cn}	Output voltage from the amplifier due to square-wave current plus system noise.
e_n	Output voltage from the amplifier due to system noise.
e_s	Output voltage from the amplifier due to velocity fluctuations on the hot wire.
e_{sc}	Output voltage from the amplifier due to velocity fluctuations plus square-wave current.
e_{scn}	Same as e_{sc} plus system noise.
e_{sn}	Same as e_s plus system noise.
e_w	Hot-wire voltage before amplification.
F	Function expressing cooling effect on hot wire by velocity and pressure of stream.
F'	Defined as $\frac{\partial F}{\partial V_p}\Big\|_p$, the derivative of F with respect to velocity at constant P.
$\overline{F}$	Time-average value of F.

NOMENCLATURE

$\underline{A}$	Time-average value of $\underline{\gamma}$.
$\underline{A}_1$	Instantaneous value of $\underline{\gamma}$ minus average value of $\underline{\gamma}$, or $\underline{A}_1 = \underline{\gamma} - \underline{A}$.
$\underline{a}$	Acceleration of vehicle.
a_{ac}	Acceleration of vehicle in feet per second per second.
a_{dc}	Acceleration of vehicle in miles per hour per second.
a_{max}	Rate of a_{dc} when steering motor is running.
a_{ms}	Instant voltage drop due to multiplier due to velocity times acceleration of vehicle.
a_{vs}	Instant voltage drop due to multiplier due to velocity times velocity of vehicle.
a_0	Output voltage from the multiplier due to steering motor.
a_{00}	Instant voltage from the multiplier in steering-gear control plus steering motor.
a'	Instant voltage from the multiplier in steering-gear control plus steering motor.
B	Voltage (general).
b_m	Rate of change, until at 0.007 inch.
C	Rate of change.
C_1, C_2	Constants.
C_3	Total capacity at input to amplifier (farads).
c	Input capacity of amplifier.
c_1	Input capacity.
D	Distance.
d	Diameter of wheel.
E	Voltage.
E_1	Voltage drop due to resistance.
E_2	Voltage drop due to capacity.
E_3	Voltage drop due to inductance.
E_4	Voltage drop due to resistance and capacity.
E_5	Voltage drop due to resistance and inductance.
E_6	Voltage drop due to capacity and inductance.
E_7	Voltage drop due to resistance, capacity, and inductance.
E_{ac}	Voltage drop due to acceleration.
E_{dc}	Voltage drop due to deceleration.
E_{ms}	Voltage drop due to motor.
E_{vs}	Voltage drop due to velocity.
e	Voltage.
e_0	Output voltage.
e_1	Input voltage.
e_2	Output voltage.
e_3	Voltage drop due to inductance.
e_4	Voltage drop due to resistance and capacity.
e_5	Voltage drop due to resistance and inductance.
e_6	Voltage drop due to capacity and inductance.
e_7	Voltage drop due to resistance, capacity, and inductance.
F	Force.
f	Frequency.
G	Gain.
g	Acceleration due to gravity.
H	Height.
h	Height.
I	Current.
I_1	Current in primary.
I_2	Current in secondary.
I_3	Current in tertiary.
i	Instantaneous current.
i_1	Instantaneous current in primary.
i_2	Instantaneous current in secondary.
i_3	Instantaneous current in tertiary.
J	Moment of inertia.
K	Constant.
K_1	Constant.
K_2	Constant.
K_3	Constant.
K_4	Constant.
K_5	Constant.
K_6	Constant.
K_7	Constant.
K_8	Constant.
K_9	Constant.
K_{10}	Constant.
K_{11}	Constant.
K_{12}	Constant.
K_{13}	Constant.
K_{14}	Constant.
K_{15}	Constant.
K_{16}	Constant.
K_{17}	Constant.

f Instantaneous deviation value of F from $\bar{F}$.

H Rate of heat loss from the hot wire per unit length.

h Fluid enthalpy per unit mass.

I Hot-wire DC current.

$\bar{I}$ Time-average of I.

I' Defined as $\frac{\partial I}{\partial V_p}\Big|_p$, the derivative of hot-wire current with respect to velocity at constant pressure.

i Instantaneous deviation value of I from $\bar{I}$.

i_s Instantaneous deviation value of hot-wire current due to imposed square-wave.

I_a, I_b Hot-wire DC current of wires a and b.

J_1 Amplifier multiplier coefficient of e_w.

J_2 Amplifier multiplier coefficient of time derivative of e_w.

K_1 Meter constant.

k Coefficient of thermal conductivity.

L Length of hot-wire.

M Meter reading of true RMS voltage.

$M_c, M_{cn}, M_n, M_s, M_{sc}, M_{scn}, M_{sn}$ Meter readings corresponding to voltages, e, with same subscripts.

N_{Pr} Prandtl number, equals $c_p \mu/k$.

N_{Re} Reynolds number, equals $\mu \bar{U} D/\rho$.

P Pressure of fluid in the boundary layer.

$\bar{P}$ Time-average of P.

p Instantaneous deviation value of P from $\bar{P}$.

P^* Pressure of fluid, units of atmospheres.

q Rate of heat transfer per unit time.

R Hot-wire resistance.

$\bar{R}$ Time-average of R.

r	Instantaneous deviation value of hot-wire resistance from $\bar{R}$.
R_e	Resistance of wire in equilibrium with ambient fluid temperature, T_e.
$\bar{R}_e$	Time-average value of R_e.
r_e	Instantaneous deviation value of R_e from $\bar{R}_e$.
R_g	Resistance of wire in equilibrium with fluid temperature, T_g.
$\bar{R}_g$	Time-average value of R_g.
r_g	Instantaneous deviation value of R_g from $\bar{R}_g$.
R_o	Resistance of wire at reference temperature, T_o.
T	Temperature.
$\bar{T}$	Time-average of T.
t	Instantaneous deviation value of T from $\bar{T}$.
T_e	Ambient temperature of the stream entering the tunnel.
T_g	Temperature of fluid at a point in the boundary layer.
$\bar{T}_g$	Time-average value of T_g.
T_o	An arbitrary reference temperature for computing resistance of wire material, handbook value.
T_s	Surface temperature of the heated plate.
T_w	Hot-wire temperature.
T	Temperature of the fluid in the free stream.
U	Velocity of the fluid in the x-direction.
$\bar{U}$	Time-average value of U.
u	Instantaneous deviation value of U from $\bar{U}$.
U	Velocity of the fluid in the free stream.
V	Velocity of the fluid in the y-direction.
$\bar{V}$	Time-average of V.
v	Instantaneous deviation value of V from $\bar{V}$.

v	Instantaneous deviation value of V from $\bar{V}$.
$\bar{V}$	Time-average of V.
V	Velocity of the fluid in the y-direction.
U	velocity of the fluid in the free stream.
u	Instantaneous deviation value of U from $\bar{U}$.
$\bar{U}$	Time-average value of U.
X	Velocity of the fluid in the x-direction.
T	Temperature of the fluid in the free stream.
T_w	Wall-area temperature.
T_s	Surface temperature of the heated plate.
T_o	An arbitrary reference temperature for computing resistance of wire material, usually 0°C value.
$\bar{T}_w$	Time-average value of T_w.
T_f	Temperature of fluid at a point in the boundary layer.
T_a	Ambient temperature of the stream entering the tunnel.
t	Instantaneous deviation value of T from $\bar{T}$.
$\bar{T}$	Time-average of T.
T	Temperature.
h_w	Resistance of wire at temperature, T_w.
R_o	Resistance deviation value of R_w from $\bar{R}_w$.
$\bar{R}_w$	Time-average value of R_w.
K_w	Resistance of wire in application with fluid temperature, T_w.
E_w	Time-average value of E_w.
e_w	Instantaneous deviation value of E_w from $\bar{E}_w$.
K_w	Resistance of wire in application with fluid temperature, T_w.
x	Instantaneous deviation value of X from $\bar{X}$.

V_a, V_b Velocity of fluid perpendicular to wires A and B.

V_θ Velocity of fluid at angle θ from perpendicular to wire.

V_p General velocity perpendicular to wire.

v_p General deviation value of V_p from its time-average.

V^* Velocity of fluid in units of 100 ft/sec.

W Velocity of fluid in z-direction.

$\bar{W}$ Time-average value of W.

W_i Rate at which work is done on a particle of fluid due to external fields.

W_f Rate at which work is done against viscous stresses.

X, Y, Z Body forces in the x-, y-, and z-directions.

x, y, z Distances in the direction of mean flow, perpendicular to the plate and transverse to the plate.

α_e Temperature coefficient of resistivity at T_e.

α_g Temperature coefficient of resistivity at T_g.

α_o Temperature coefficient of resistivity at T_o.

α Thermal diffusivity, equals $k/\rho c_p$.

γ Resistance ratio, resistance of hot wire to resistance of cold wire.

ε_h Coefficient of eddy heat (or energy) transfer.

ε_m Coefficient of eddy momentum transfer.

θ Angle between perpendicular to wire and mean velocity vector.

μ Viscosity.

ν Kinematic viscosity.

ρ Density.

τ Time.

Appendix B

BOUNDARY LAYER EQUATIONS

The general equations for viscous, constant-property fluid flow are quoted below. The Navier-Stokes equations of momentum and continuity in rectangular coordinates are:

Momentum:

$$\rho \frac{DU}{D\tau} = -\frac{\partial P}{\partial x} + \rho X + \mu \left[\nabla^2 U + \frac{1}{3} \frac{\partial}{\partial x} (\nabla \cdot \vec{V}) \right]$$

$$\rho \frac{DV}{D\tau} = -\frac{\partial P}{\partial y} + \rho Y + \mu \left[\nabla^2 V + \frac{1}{3} \frac{\partial}{\partial y} (\nabla \cdot \vec{V}) \right] \tag{8}$$

$$\rho \frac{DW}{D\tau} = -\frac{\partial P}{\partial z} + \rho Z + \mu \left[\nabla^2 W + \frac{1}{3} \frac{\partial}{\partial z} (\nabla \cdot \vec{V}) \right]$$

Continuity:

$$\frac{\partial \rho}{\partial \tau} + \frac{\partial}{\partial x}(\rho U) + \frac{\partial}{\partial y}(\rho V) + \frac{\partial}{\partial z}(\rho W) = 0 \tag{9}$$

The energy equation is:

$$\frac{\partial}{\partial x}\left(k \frac{\partial T}{\partial x}\right) + \frac{\partial}{\partial y}\left(k \frac{\partial T}{\partial y}\right) + \frac{\partial}{\partial z}\left(k \frac{\partial T}{\partial z}\right) + W_i + W_f = \rho \frac{Dh}{D\tau} - \frac{DP}{D\tau} \tag{10}$$

where W_i is the rate at which work is done on a particle of fluid by an external field and W_f is the rate at which work is done against viscous stresses. Also, $D/D\tau$ represents the substantial derivative defined as

$$\frac{D}{D\tau} \equiv \frac{\partial}{\partial \tau} + \frac{\partial}{\partial x} + \frac{\partial}{\partial y} + \frac{\partial}{\partial z}$$

The Navier-Stokes equations are simplified by assuming two-dimensional, steady, incompressible flow in the absence of body forces for an ideal fluid of constant viscosity and thermal conductivity. Prandtl's order-of-magnitude treatment further reduces them until the result is:

$$U \frac{\partial U}{\partial x} + V \frac{\partial U}{\partial y} = -\frac{1}{\rho} \frac{\partial P}{\partial x} + \nu \frac{\partial^2 U}{\partial y^2} \tag{11}$$

$$\eta \frac{\partial \chi}{\partial \eta} + \lambda \frac{\partial^2}{\partial \eta} = -\frac{b}{1} \frac{\partial \chi}{\partial b} + \nu \frac{\partial^3 \rho_2}{\partial_2 \eta} \tag{11}$$

defining kinematic pressure (how well the density is:

Ility of constant viscosity and thermal conductivity). Prandtl's celebrated "boundary layer" approximation (that is the essence of many flows for at least

The Navier-Stokes equations can simplified by assuming two-dimensional steadiness. Also, D/Dt represents the substantial derivative defined as

$$\frac{D}{D} = \frac{\partial}{\partial} + \frac{\partial}{\partial} + \frac{\partial}{\partial} + \frac{\partial}{\partial}$$

external field and f^i is the rate at which work is done on a particle of fluid by an where M^i is the rate at which work is done on a particle of fluid by an

$$\frac{\partial}{\partial}\left(\rho \frac{\partial}{\partial t}\right) + \frac{\partial}{\partial}\left(\rho \frac{\partial}{\partial t}\right) + \frac{\partial}{\partial}\left(\rho \frac{\partial}{\partial t}\right) + M^i + M^i = b \frac{D}{D} - \frac{D}{D} \tag{10}$$

The energy equation is:

$$\frac{\partial}{\partial} + \frac{\partial}{\partial}(b) + \frac{\partial}{\partial}(b) + \frac{\partial}{\partial}(b) = 0 \tag{9}$$

Continuity:

$$b \frac{D}{D} = -\frac{\partial}{\partial} + b + \left[\frac{1}{3} \frac{\partial}{\partial} (\nabla \cdot \underline{v}) \right]$$

$$b \frac{D}{D} = -\frac{\partial}{\partial} + b + \left[\frac{1}{3} \frac{\partial}{\partial} (\nabla \cdot \underline{v}) \right] \tag{8}$$

$$b \frac{D}{D} = -\frac{\partial}{\partial} + b + \left[\frac{1}{3} \frac{\partial}{\partial} (\nabla \cdot \underline{v}) \right]$$

Momentum:

The general equations for viscous, compressible fluid flow are named below. The Navier-Stokes equations of motion-cit is

Appendix A

Governing Fluid Dynamics

and

$$\frac{\partial U}{\partial x} + \frac{\partial V}{\partial y} = 0 \tag{12}$$

for application to the boundary layer of a flat plate.

Similarly, the energy equation can be written in a simpler form as

$$U\frac{\partial T}{\partial x} + V\frac{\partial T}{\partial y} = \frac{k}{\rho c_p}\frac{\partial^2 T}{\partial y^2} + \frac{\mu}{\rho c_p}\left(\frac{\partial U}{\partial x}\right)^2 \tag{13}$$

The last term, $\frac{\mu}{\rho c_p}\left(\frac{\partial U}{\partial x}\right)^2$, is usually considered negligible.

Thus the three equations of importance are:

Momentum:

$$U\frac{\partial U}{\partial x} + V\frac{\partial U}{\partial y} = -\frac{1}{\rho}\frac{\partial P}{\partial x} + \nu\frac{\partial^2 U}{\partial y^2} \tag{14}$$

Continuity:

$$\frac{\partial U}{\partial x} + \frac{\partial V}{\partial y} = 0 \tag{15}$$

Energy:

$$U\frac{\partial T}{\partial x} + V\frac{\partial T}{\partial y} = \alpha\frac{\partial^2 T}{\partial y^2} \tag{16}$$

with boundary conditions

$$\text{(a) at } y = 0: \quad T = T_s \text{ or } \frac{\partial T}{\partial y} = -\frac{\dot{q}}{kA} \quad \text{and} \quad U = 0$$
$$\text{(b) at } y = \infty: \quad T = T_\infty \quad \text{and} \quad U = U_\infty \tag{17}$$

Multiplying the continuity equation by U, adding the result to the momentum equation; and multiplying the continuity equation by T, adding the result to the energy equation, then simplifying both gives

$$\frac{\partial}{\partial x}(P + \rho U^2) = \frac{\partial}{\partial y}\left(\mu\frac{\partial U}{\partial y} - \rho UV\right) \tag{18}$$

$$\frac{\partial}{\partial x}(UT) = \frac{\partial}{\partial y}\left(\alpha\frac{\partial T}{\partial y} - VT\right) \tag{19}$$

and

$$\frac{\partial}{\partial x}\left(\frac{\partial \lambda}{\partial N}\right) + \frac{\partial}{\partial A}\left(\frac{\partial \lambda}{\partial N}\right) = 0 \tag{12}$$

the application to the boundary layer of a flat plate.

Similarly, the energy equation can be written in a similar form as

$$U\frac{\partial \lambda}{\partial x} + V\frac{\partial \lambda}{\partial I} = \frac{bc^b}{k}\frac{\partial \lambda_s}{\partial I^2} + \frac{bc^b}{k}\left(\frac{\partial N}{\partial x}\right)_s \tag{13}$$

The last term, $\frac{bc^b}{k}\left(\frac{\partial x}{\partial N}\right)_s$, is usually considered negligible.

Thus the three equations of importance are:

Momentum:

$$U\frac{\partial U}{\partial x} + V\frac{\partial U}{\partial N} = -\frac{b}{l}\frac{\partial x}{\partial P} + \nu\frac{\partial N^2}{\partial^2 U} \tag{14}$$

Continuity:

$$\frac{\partial x}{\partial U} + \frac{\partial N}{\partial A} = 0 \tag{15}$$

Energy:

$$U\frac{\partial x}{\partial I} + V\frac{\partial I}{\partial \lambda} = \epsilon\frac{\partial N_s^2}{\partial^2 I} \tag{16}$$

with boundary conditions

(a) at $\lambda = 0$: $T = T_0$ or $\frac{\partial I}{\partial \lambda} = -\frac{\lambda}{kA}$ and $U = 0$ (17)

(b) at $\lambda = \infty$: $T = T_\infty$ and $U = U_\infty$

Multiplying the continuity equation by U, adding the result to the momentum equation, and multiplying the continuity equation by V, adding the result to the energy equation, then simplifying each gives

$$\frac{\partial}{\partial x}(\rho U^2) = \frac{\partial}{\partial N}\left(\mu\frac{\partial U}{\partial N} - \rho UV\right) \tag{18}$$

$$\frac{\partial}{\partial x}(UT) = \frac{\partial}{\partial N}\left(\epsilon\frac{\partial I}{\partial N} - VT\right) \tag{19}$$

In turbulent flow Reynolds assumed that all quantities are made up of an average value plus a superposed fluctuation component such that

$$U = \bar{U} + u$$
$$V = \bar{V} + v$$
$$T = \bar{T} + t \qquad (20)$$
$$P = \bar{P} + p$$

Substituting these in equation (18) and (19), multiplying out and taking time averages:

$$\frac{\partial}{\partial x}\left(\bar{P} + \rho\bar{U}^2 + \rho\overline{u^2}\right) = \frac{\partial}{\partial y}\left(\mu\frac{\partial \bar{U}}{\partial y} - \rho\,\bar{U}\bar{V} - \rho\,\overline{uv}\right) \qquad (1)$$

$$\frac{\partial}{\partial x}\left(\bar{U}\bar{T} + \overline{ut}\right) = \frac{\partial}{\partial y}\left(\alpha\frac{\partial \bar{T}}{\partial y} - \bar{V}\bar{T} - \overline{vt}\right) \qquad (2)$$

In general $\overline{uv}$ and $\overline{vt}$ may be expected to have values other than zero as argued below: The $\bar{U}$ velocity profile in a boundary layer over a flat plate is as shown in the sketch, Fig. 5. Chosing a point at x,y: If a 'packet' of air goes by the point in a + V direction, air from closer to the plate will be forced into the 'hole' left by the packet. On the average, the entering air will have a U-velocity less than that which is average for the point x,y. This corresponds to a (-u) as observed at that point.

Conversely, movement of a packet in the (-v) direction gives rise to a (+u) velocity.

Consequently, where there is a gradient of $\bar{U}$, a (+v) produces a (-u) and a (-v) produces a (+u), therefore the product is negative on the average. u and v are said to be 'cross-correlated' such that

$$\overline{uv} = \lim_{\tau\to\infty} \frac{1}{2\tau}\int_{-\tau}^{+\tau} (uv)\,d\tau \qquad (23)$$

$$\overline{\Pi A} = \lim_{t\to\infty} \frac{\pi\lambda}{t} \int_{-\lambda}^{+\lambda} (\pi\nu)\, d\chi \qquad (12)$$

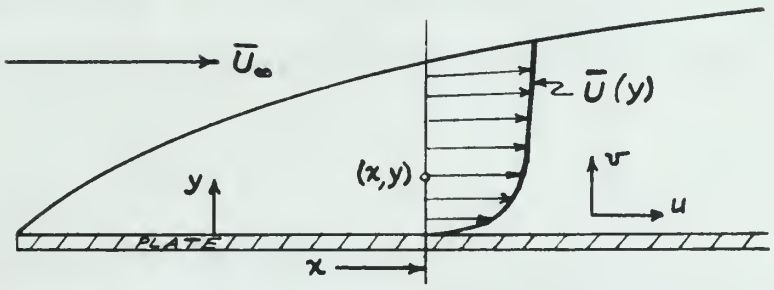

Fig. 5. Velocity Profile

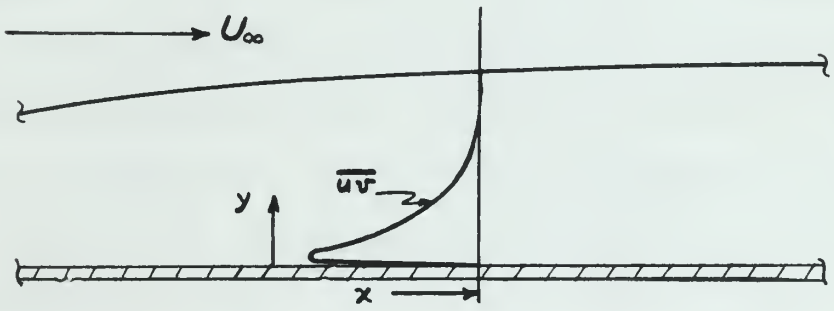

Fig. 6. Velocity Correlation Profile

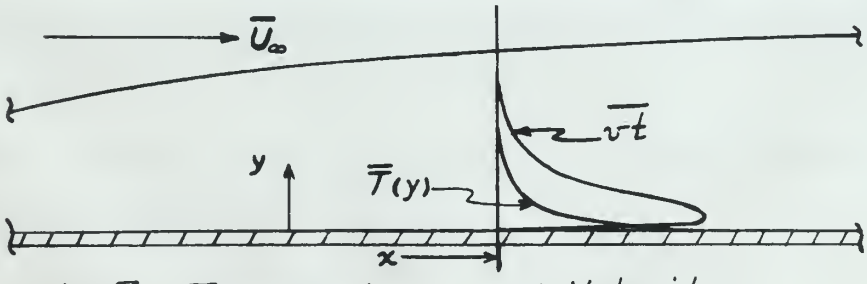

Fig. 7. Temperature and Velocity-Temperature Correlation Profiles

Close to the plate the fluid becomes laminar in the sub-layer, so u and v tend to zero. At the edge of the boundary layer where the gradient of U disappears, u and v tend to cross-correlate in a random fashion so the average is zero.

In summary, the expected behavior of $\overline{uv}$ as a function of y should appear as shown in Fig. 6. Parallel reasoning leads one to expect a positive correlation of $\overline{vt}$ where there is a gradient of $\overline{T}$ such that

$$\overline{vt} = \lim_{\tau \to \infty} \frac{1}{2\tau} \int_{-\tau}^{+\tau} (vt)\, d\tau \tag{24}$$

These results are sketched in Fig. 7.

There is also a gradient of temperature in the x-direction producing a $\overline{ut}$ correlation, but usually the gradient of $\overline{T}$ in the x-direction is much smaller than in the y-direction, fluctuations in T are smaller, so $\overline{ut}$ is expected to be an order of magnitude smaller than $\overline{vt}$. Johnson in reference (1) does show results, however, that indicate $\overline{ut}$ to be about twice the magnitude of $\overline{vt}$. In this thesis $\overline{ut}$ cnacels out of the formulas used to calculate $\overline{vt}$. Its order of magnitude compared to $\overline{vt}$ is therefore not determined.

It must be remembered that near the 'edge' of the thermal boundary layer $\overline{ut}$ and $\overline{vt}$ could become comparable; however the methods of measurement are unlikely to detect these quantities with much certainty near the free stream.

The concepts of eddy shear stress coefficient and eddy energy coefficient are defined by:

$$\overline{uv} = -\varepsilon_m \frac{\partial \bar{U}}{\partial y} \tag{3}$$

and

$$\overline{vt} = -\varepsilon_h \frac{\partial \bar{T}}{\partial y}$$

and

$$\overline{uv} = -\varepsilon_m \frac{\partial \bar{u}}{\partial y} \tag{2}$$

$$\overline{v\xi} = -\varepsilon_h \frac{\partial \bar{\xi}}{\partial y}$$

The coupling of eddy viscosity coefficients and eddy conductivity mentioned are valid in order these quantities with much uncertainty under flow systems.

It must be remembered that even the 'edge' of the thermal boundary layer $\bar{u}\bar{v}$ and $\bar{v}\bar{\xi}$ could become considerably; however the methods of measurement are not defined by

(4)

where ε_m and ε_h are probably different functions of y.

When these definitions are substituted in equations (1) and (2), the result is

$$\frac{\partial}{\partial x}\left(\bar{P}+\rho\bar{U}^2+\rho\overline{u^2}\right) = \frac{\partial}{\partial y}\left[\left(\mu+\rho\varepsilon_m\right)\frac{\partial\bar{U}}{\partial y} - \bar{U}\bar{V}\right] \tag{25}$$

and

$$\frac{\partial}{\partial x}\left(\bar{U}\bar{T}+\overline{ut}\right) = \frac{\partial}{\partial y}\left[\left(\alpha+\varepsilon_h\right)\frac{\partial\bar{T}}{\partial y} - \bar{V}\bar{T}\right] \tag{26}$$

Solutions to these equations have been obtained for various simple geometries and assumed empirical distributions of pressure, velocity and temperature. In most cases the ratio of ε_m to ε_h is assumed to be constant or some arbitrary function of y. Very few measurements of ε_m and ε_h are available.

$$\left[\bar{V}\bar{U} - \frac{\bar{\nu}}{g}\left(\varepsilon'' + \frac{g}{\partial \bar{z}}\right)\right]\frac{g}{\partial^2} = \left(\bar{\mu} + \bar{U}\right)\frac{g}{\partial x}$$

(28)

$$\left[\bar{V}\bar{U} - \frac{\bar{\nu}}{g}\left(\varepsilon'' + \frac{g}{\partial \bar{z}}\right)\right]\frac{g}{\partial^2} = \left(\bar{\mu} + \bar{U}_s + b\varepsilon_m\right)\frac{g}{\partial x}$$

(29)

Appendix C*

HOT WIRE ANEMOMETER THEORY

A. Steady Flow.

Hot-wire theory has been well developed for various ideal cases. Most of the theory is based on King's equation which appears in various forms such as

$$\frac{H}{k(T_w - T_e)} = C_3 + C_4\sqrt{N_{Pr}\,N_{Re}} \tag{27}$$

or alternatively

$$H = (T_w - T_e)\left[C_3 k + C_4\sqrt{N_{Pr}}\sqrt{\frac{k^2\rho}{\mu}}\sqrt{V_p D}\right] \tag{28}$$

For a gas, ρ is proportional to P/T_g, and for air $k^2/\mu T_g$ is approximately independent of pressure and temperature such that

$$H = (T_w - T_e)\,F(PV_p) \tag{29}$$

where

$$F(PV_p) = \left[0.58 + 6.6\sqrt{P^* V^* D^*}\right] \tag{30}$$

The Flow Corporation, Cambridge, Massachusetts supplies hot-wire anemometer equipment which makes use of several interesting techniques. First, the equipment is of the 'constant current' type. Second, all measurements are made with the hot wire at a selected resistance ratio above the cold wire resistance. Third, measurements of unknown signals from the wire are made relative to a known square-wave signal applied to the wire from an internal circuit.

A summary of the principles of wire theory will give adequate under-

---

* This appendix is bases primarily of references (3) and (12).

Appendix C*

Gas Flow Measuring Devices

V. Steady Flow.

One-dimensional flow may also be analyzed for various other cases. When of the channel is caused by a constriction which changes its velocity there may be

$$\frac{p(z^n - z^0)}{n} = c_1^2 + c^2 \sqrt{\quad} \tag{19}$$

or alternatively

$$R = (z^n - z^0)\left[c_1^2 + c^2 \sqrt{\quad}\right] \tag{13}$$

Now c for z_1 is determined to $p_1^{1/n}$ and for all $z_2 \neq z_1$ it incrementally independent of pressure and temperature such that

$$R = (z^n - z^0)\,k(R_1^2) \tag{20}$$

where

$$k(R_1^2) = \left[0.20 + 1.1\sqrt{\quad}\right] \tag{20}$$

The flow coefficient, Cavitation, incompressible swelling hot-spin be-
ometer schemes which cause use of several interacting variables.
Pitot, the reference is of the 'constant external' type. Remove, all
measurements are made with the box axis at a selected orientation ratio
above the real axis restriction. Total measurements of minimum stagnia
from the axis are made relative to a known 'zero-axis' signal applied to
the main flow as internal circuit.

* This appendix is based primarily on reference (3) and (12).

V measure of the principles of wire theory will give velocity measure-

standing of wire operation.

For a hypothetical fluctuating flow, the power input to the wire balances the power carried away by the stream,

$$I^2R = H\,L = (T_w - T_e)\,L\,F(PV_p) \tag{31}$$

Also, neglecting second order terms,

$$R = R_o\left[1 + \alpha_o(T_w - T_o)\right] \tag{32}$$

where R_o, α_o, and T_o are arbitrary corresponding quantities. These can be chosen as R_e, α_e and T_e at the 'cold' temperature of the wire assumed to be in equilibrium with the stream ambient temperature. Therefore

$$R = R_e\left[1 + \alpha_e(T_w - T_e)\right] \tag{33}$$

Solving (33) for $(T_w - T_e)$ and making use of $\gamma = R/R_e$, equation (31) becomes

$$I^2 \qquad (1 - \frac{1}{\gamma}) \frac{L\,F(PV_p)}{\alpha_e R_e} \tag{34}$$

In steady state, therefore, a measurement of I will give the PV_p product since all other quantities are fixed. In practice for a particular wire at low velocities, a calibration of I vs V_p is made assuming P is nearly constant. Because it usually results in a straight line, the calibration is usually plotted as I^2 vs $\sqrt{V_p}$ giving a graph that may be represented by an equation of the form

$$I^2 = C_1 + C_2\sqrt{V_p} \tag{35}$$

The derivative with respect to velocity is

$$\frac{dI}{dV_p} = \frac{C_2}{4\,I\sqrt{V_p}} \tag{36}$$

In Flow Corporation literature, the quantity dI/dV_p is denoted by I'.

$$\frac{dP}{dI} = \frac{V \pm \sqrt{\quad}}{2} \tag{36}$$

The derivative will respect to velocity is

$$I_2 = C^1 + C^2 \sqrt{\quad} \tag{38}$$

replacement by an expression of the form

$$\frac{1}{2} (1 - \frac{\beta}{\quad}) \frac{\quad}{\quad} \tag{40}$$

In steady state, therefore, a measurement of I will give the P^1 product times all other quantities are fixed. In practice the ϵ particles play no at low velocities, a calibration of I vs λ^1 is made allowing γ to vary. Because it usually results in a straight line, the calibration is usually plotted as I_2 vs λ^1 giving $\sqrt{\quad}$ which can be replaced by an expression of the form

$$I_2 = C^1 + C^2 \sqrt{\quad} \tag{38}$$

The derivative with respect to velocity is

$$\frac{dP}{dI} = \frac{V \pm \sqrt{\quad}}{2} \tag{36}$$

In Flow Calorimetry, the quantity $\gamma(\Delta H)^1$ is denoted by ϵ',

$$I_2 = K \epsilon' = (T^{\circ} - T_0^{\circ}) \rho \gamma(\Delta H_0^{\circ}) \tag{31}$$

Also, neglecting second order terms,

$$T = T_0^{\circ} \left[1 + \alpha_{\epsilon}(T^{\circ} - T_0^{\circ}) \right] \tag{32}$$

where T°, $\alpha_{\epsilon}^{\circ}$, and T_0° are arbitrary corresponding quantities. These can be chosen as T°, $\alpha_{\epsilon}^{\circ}$ and T_0° of the 'real' temperature of the wire assumed to be in equilibrium with the stream ambient temperature. Therefore

$$R = R^{\circ} \left[1 + \alpha_{\epsilon}^{\circ}(T^{\circ} - T_0^{\circ}) \right] \tag{33}$$

Solving (33) for $(T^{\circ} - T_0^{\circ})$ and making use of $\epsilon = \gamma/\rho^{\circ}$, equation (11) becomes

B. Turbulent Flow.

When the stream is turbulent, no steady state exists and the operation of the wire must be analyzed from a time dependent approach. The wire stores heat. Since it cannot change heat storage instantaneously, a power loss balance for the wire is

$$cAL \frac{\partial T_w}{\partial \tau} = I^2R - \frac{L(\gamma - 1)}{\alpha_e} F(PV_p) \tag{37}$$

From equation (33)

$$\frac{\partial T_w}{\partial \tau} = \frac{1}{\alpha_e R_e} \frac{\partial R}{\partial \tau} \tag{38}$$

Take $R = \bar{R} + r$ (39)

and $F(PV_p) = F(\bar{P}\bar{V}_p + \bar{P}v_p)$ (40)

where also

$$F(\bar{P}\bar{V}_p + \bar{P}v_p) = F(\bar{P}\bar{V}_p) + \left.\frac{\partial F}{\partial V_p}\right]_P v_p = \bar{F}(PV_p) + F' v_p \tag{41}$$

Substituting these in equation (37), expanding and subtracting the steady state equation (31) leaves

$$c A L \frac{\partial r}{\partial \tau} = \alpha_e R_e I^2 r - L(\bar{R} - R_e) F' v_p - L \bar{F} r \tag{42}$$

Since the voltage across the wire is

$$e_w = I r \tag{43}$$

equation (42) becomes

$$c A L \frac{d e_w}{d \tau} = \left[\alpha_e R_e I^2 - L\bar{F}\right] e_w - L(\bar{R} - R_e) I F' v_p \tag{44}$$

Solving for v_p:

$$v_p = -\left[\frac{L\bar{F} - \alpha_e R_e I^2}{L(\bar{R} - R_e) I F'} e_w + \frac{c A L}{L(\bar{R} - R_e) I F'} \frac{d e_w}{d \tau}\right] \tag{45}$$

Thus, the fluctuating velocity component, v_p, is a function of the voltage and the time derivative of the voltage induced in the wire by the velocity. The Flow Corporation HWB performs this operation such that the

8. Surplus Flow.

When the stocks in question, as already given values and the change of the value must be analyzed into a time dependent element. The value stocks have. Since it cannot change that according instantaneously, a power loss inheres for the wire is

$$\frac{dW}{dt} = \frac{\partial S}{\partial t^a} = I^2 R - \frac{q\epsilon}{I\,(2-1)} \qquad (33)$$

From equation (33)

$$\frac{\partial S}{\partial t^a} = \frac{q\epsilon\, x^a}{I} \frac{\partial x}{\partial t} \qquad (34)$$

Then $\qquad P = \bar{x} + x \qquad (36)$

and $\qquad \gamma(\Delta x^b) = g(\bar{x}\bar{x}^b + \bar{x}x^b) \qquad (40)$

where now

$$\gamma(\bar{x}\bar{x}^b + \bar{x}x^b) = g(\Delta\bar{x}^b) + \left[\frac{\partial s}{\partial t}\right]^b \lambda^b = \bar{x}(\Delta x^b) + \bar{x}_i \lambda^b \qquad (41)$$

Substituting these in equation (37), expanding and subtracting the steady state equation (32) leaves

$$\epsilon\,\gamma\, I \frac{\partial s}{\partial x} = q\epsilon\, x^a\, I_2 x^2 - \epsilon\,(\bar{x} - \bar{x}^b)\,\bar{x}_i\,\lambda^b - \gamma\,\bar{x}\,\lambda \qquad (42)$$

Since the voltage across the wire is

$$e^a = I\,\gamma \qquad (43)$$

equation (42) becomes

$$\epsilon\,\gamma\, I \frac{\partial s}{\partial e^a} = \left[q\epsilon\, x^a I_2 - \epsilon\right] e^a - \epsilon\,(\bar{x} - \bar{x}^b)\, I\, \bar{x}_i\, \lambda^b \qquad (44)$$

Solving for λ^b,

$$\lambda^b = -\left[\frac{I\,(q\epsilon - q\epsilon^a\, I_2}{I\,\bar{x} - q\epsilon^a\, I_2} e^a + \frac{I\,(\bar{x} - \bar{x}^b)\, I\, \bar{x}_i}{\epsilon\,\gamma\, I}\, \frac{\partial s}{\partial e^a}\right] \qquad (45)$$

Thus, the discounting relevant commodity, λ^b, is a function of the voltage and the time derivative of the voltage induced in the wire by the velocity. The flow characteristics can therefore also operation may that the

output voltage is

$$e_s = J_1 e_w + J_2 \frac{d e_w}{d \tau} \tag{46}$$

J_2 is a constant but J_1 is adjustable so that

$$J_1 = J_2 \left(\frac{L \bar{F} - \mathcal{L}_e R_e I^2}{c A L} \right) \tag{47}$$

Solving (45) for e_w or $d e_w / d\tau$ and substituting in (46)

$$e_s = -\left[\frac{J_1 L (\bar{R} - R_e) I F'}{L \bar{F} - \mathcal{L}_e R_e I^2} \right] v_p = -\left[\frac{J_2 I (\bar{R} - R_e) F'}{c A} \right] v_p , \tag{48}$$

if equation (47) is true. The adjustment of the ratio of J_1 / J_2 is made by observing the amplifier output on an oscilloscope when a square-wave current is fed to the wire. The process of 'compensating' the amplifier is detailed in Appendix D. At the point of proper compensation with the wire in still air, the wire response to the square-wave current is

$$e_c = \left[\frac{2 J_1 \bar{I}^2 \bar{R} R_e \mathcal{L}_e}{L \bar{F} - \bar{I}^2 \mathcal{L}_e R_e} \right] i_s = \left[\frac{2 J_2 \bar{I}^2 \bar{R} R_e \mathcal{L}_e}{c A L} \right] i_s \tag{49}$$

where $$I = \bar{I} + i_s \tag{50}$$

The ratio of e_s to e_c is

$$\frac{e_s}{e_c} = \left[\frac{L (\bar{R} - R_e) I F'}{2 \bar{I}^2 \bar{R} R_e \mathcal{L}_e i_s} \right] v_p \tag{51}$$

Since $$F' = \frac{2 \mathcal{L}_e R_e}{L} \left(\frac{\gamma}{\gamma - 1} \right) \bar{I} I' \tag{52}$$

then $$\frac{e_s}{e_c} = \frac{I'}{i_s} v_p , \text{ or } v_p = \frac{i_s}{I'} \frac{e_s}{e_c} \tag{53}$$

It must be realized that in the derivation of all equations, fluctuating components are small compared with the average values. This allows neglecting second-order products of the fluctuating components as being immeasurably small. Even when this is not strictly true, the method of normalizing represented by equation (51) compensates for some deviation.

C. Turbulent Flow with Temperature Fluctuations.

A fluid in turbulent flow past a heated surface will become heated in some fluctuating manner. The effect of varying fluid temperature may be regarded as a change in the 'cold' resistance of the wire, R_g, such that

$$R_g = \bar{R}_g + r_g \tag{54}$$

$$= R_g \left[1 + \alpha_g (T_g - T_a) \right] \tag{55}$$

Combining these with the power balance equations in the presence of velocity fluctuations, plus the relations

$$e_w = I r$$

$$e_s = J_1 \left(e_w + \frac{c A L}{L \bar{F} - \bar{I}^2 \alpha_g R_g} \frac{d e_w}{d \tau} \right)$$

$$e_c = \left(\frac{2 J_1 \bar{I}^2 \bar{R} R_g \alpha_g}{L \bar{F} - \bar{I}^2 R_g \alpha_g} \right) i_s$$

$$F' = \frac{2 \bar{I} I' \alpha_g R_g}{L} \frac{\bar{R}}{\bar{R} - \bar{R}_g}, \quad \text{and}$$

$$F(PV_p) = \frac{\alpha_g R_g \bar{I}^2 \bar{R}}{L (\bar{R} - \bar{R}_g)}$$

gives

$$2 i_s \frac{e_s}{e_c} + 2 I' v_p \frac{\bar{I}}{\bar{R} - \bar{R}_g} r_g = 0 \tag{56}$$

[illegible]

Noting that $$T_g = \bar{T}_g + t \tag{57}$$

$$\bar{R}_g = R_e\left[1 + \alpha_e(T_g - T_e)\right] \tag{55}$$

and

$$\tau_g = \alpha_e R_e t \tag{58}$$

leads to

$$2 i_g \frac{e_s}{e_c} + 2 I' v_p - \frac{\alpha_e \bar{I}}{\gamma - \left[1 + \alpha_e(\bar{T}_g - T_e)\right]} t = 0 \tag{59}$$

e_s and e_c have been taken as the outputs from an ideal amplifier. An actual amplifier will have an output of $(e_s + e_n)$ and $(e_c + e_n)$. When this output is fed to a true RMSvoltmeter, the latter will have a reading of

$$M_{sn} = K_1 \sqrt{\lim_{\tau \to \infty} \frac{1}{2\tau} \int_{-\tau}^{+\tau} (e_s + e_n)^2 \, d\tau} \tag{60}$$

or $$M_{cn} = K_1 \sqrt{\lim_{\tau \to \infty} \frac{1}{2\tau} \int_{-\tau}^{+\tau} (e_c + e_n)^2 \, d\tau} \tag{61}$$

But the time average of the voltage is $\overline{(e_s + e_n)^2} = \overline{e_s^2} + \overline{e_n^2}$ since the time average of $\overline{e_s e_n} = 0$. That is, there is no correlation between noise and signal.

Therefore,

$$M_{sn} = K_1 \sqrt{\overline{e_s^2} + \overline{e_n^2}} \tag{62}$$

and

$$M_n = K_1 \sqrt{\overline{e_n^2}} \tag{63}$$

It follows that $$\sqrt{M_{sn}^2 - M_n^2} = K_1 \sqrt{\overline{e_s^2}} \tag{64}$$

the RMS value of e_s. For the square-wave

$$\sqrt{M_{scn}^2 - M_{sn}^2} = K_1 \sqrt{\overline{e_c^2}} = K_1 e_c. \tag{65}$$

Squaring equation (59) and making use of the meter relations gives

$$\overline{(e_{2m}^2 - e_{1m}^2)} = \overline{e_1^2} = \overline{e_2^2} \tag{29}$$

Inserting equation (29) and noting one of the many relations given

It follows that $\overline{(e_{2m}^2 - e_{1m}^2)} = \overline{e_1^2} = \overline{e_2^2}$ (28)

the rms value of e^2. For the square-wave

$$\overline{e_{1m}^2} = \overline{e_1^2} \tag{27}$$

and

$$\overline{e_{2m}^2} = \overline{e_2^2} \tag{26}$$

Therefore,

$$\overline{e_{1m}^2} = \overline{e_1^2 + e_{2m}^2} \tag{25}$$

since the time average of $\overline{e_1 e_2} = 0$. That is, there is no correlation between noise and signal.

But the time average of the voltage is $\overline{(e_1 + e_{2m})^2} = \overline{e_1^2} + \overline{e_{2m}^2}$

or $e_{2m} = E \sqrt{\lim_{T \to \infty} \frac{1}{2T} \int_{-T}^{+T} (e_1 + e_{2m})^2 \, dt}$ (24)

$$E_{2m} = E \sqrt{\lim_{T \to \infty} \frac{1}{2T} \int_{-T}^{+T} (e_1 + e_{2m})_2 \, dt} \tag{24a}$$

The second amplifier will have an output of $\alpha(e_1 + e_{2m})$ and $\alpha(e_1 + e_{2m})$ when the square output is fed to a true Root-Mean-Square meter, the latter will have a reading of

$$E_{2m} = E \sqrt{\lim_{T \to \infty} \frac{1}{2T} \int_{-T}^{+T} (e_1 + e_{2m})_2 \, dt} \tag{24b}$$

e_1 and e_{2m} have been taken as the output from an ideal amplifier.

Inserting these values in equation (23) and solving for α

$$\alpha = \frac{E_{2m}}{\sqrt{e_1^2 + e_{2m}^2}} \tag{23}$$

Now the rms value of e_{2m} is

$$e_{2m} = \frac{4}{\pi} E \tag{22}$$

Inserting this value in equation (22) and solving for α

$$\alpha = \frac{E_{2m}}{\sqrt{e_1^2 + \frac{8}{\pi^2} E^2}} \tag{21}$$

Now the rms value of e_{2m} is

$$e_{2m} = \frac{4}{\pi} E \tag{20}$$

Inserting this value in equation (20) and solving for α

$$\alpha = \frac{E_{2m}}{\sqrt{e_1^2 + \frac{8}{\pi^2} E^2}} \tag{19}$$

Now the rms value of e_{2m} is

$$e_{2m} = \frac{4}{\pi} E \tag{18}$$

Inserting this value in equation (18) and solving for α

$$\alpha = \frac{E_{2m}}{\sqrt{e_1^2 + \frac{8}{\pi^2} E^2}} \tag{17}$$

Now the rms value of e_{2m} is

$$e_{2m} = \frac{4}{\pi} E \tag{16}$$

Inserting this value in equation (16) and solving for α

$$\alpha = \frac{E_{2m}}{\sqrt{e_1^2 + \frac{8}{\pi^2} E^2}} \tag{15}$$

Now the rms value of e_{2m} is

$$e_{2m} = \frac{4}{\pi} E \tag{14}$$

Inserting this value in equation (14) and solving for α

$$\alpha = \frac{E_{2m}}{\sqrt{e_1^2 + \frac{8}{\pi^2} E^2}} \tag{13}$$

Now the rms value of e_{2m} is

$$e_{2m} = \frac{4}{\pi} E \tag{12}$$

Inserting this value in equation (12) and solving for α

$$\alpha = \frac{E_{2m}}{\sqrt{e_1^2 + \frac{8}{\pi^2} E^2}} \tag{11}$$

Now the rms value of e_{2m} is

$$e_{2m} = \frac{4}{\pi} E \tag{10}$$

Inserting this value in equation (10) and solving for α

$$\alpha = \frac{E_{2m}}{\sqrt{e_1^2 + \frac{8}{\pi^2} E^2}} \tag{9}$$

Now the rms value of e_{2m} is

$$e_{2m} = \frac{4}{\pi} E \tag{8}$$

Inserting this value in equation (8) and solving for α

$$\alpha = \frac{E_{2m}}{\sqrt{e_1^2 + \frac{8}{\pi^2} E^2}} \tag{7}$$

Now the rms value of e_{2m} is

$$e_{2m} = \frac{4}{\pi} E \tag{6}$$

Inserting this value in equation (6) and solving for α

$$\alpha = \frac{E_{2m}}{\sqrt{e_1^2 + \frac{8}{\pi^2} E^2}} \tag{5}$$

Now the rms value of e_{2m} is

$$e_{2m} = \frac{4}{\pi} E \tag{4}$$

Inserting this value in equation (4) and solving for α

$$\alpha = \frac{E_{2m}}{\sqrt{e_1^2 + \frac{8}{\pi^2} E^2}} \tag{3}$$

Now the rms value of e_{2m} is

$$e_{2m} = \frac{4}{\pi} E \tag{2}$$

Inserting this value in equation (2) and solving for α

$$\alpha = \frac{E_{2m}}{\sqrt{e_1^2 + \frac{8}{\pi^2} E^2}} \tag{1}$$

$$(2\,i_s)^2\left[\frac{M_{sn}^2 - M_{ti}^2}{M_{scn}^2 - M_{an}^2}\right] = (2\,I')^2\overline{v_p^2} - \left\{\frac{4\quad \alpha_e\,\bar{I}\,I'}{\gamma - \left[1 + \alpha_e(\bar{T}_g - T_e)\right]}\right\}\overline{v_p t} + \left\{\frac{\alpha_e\,\bar{I}}{\gamma - \left[1 + \alpha_e(\bar{T}_g - T_e)\right]}\right\}^2\overline{t^2} \qquad (66)$$

A set of simultaneous equations can be obtained by measuring all quantities at several resistance ratios. For more than three resistance ratios the unknowns are overdetermined and the method of averages or least squares can be used to evaluate the unknowns.

D. Resolution of Velocity Components.

The foregoing analysis assumed that the velocity was perpendicular to the axis of the wire. Within 70° or more from the perpendicular, the cooling effect on the wire varies as the cosine of the angle, that is $V_\theta = V_p \cos\theta$. A wire at 45° to the average stream direction has an average effective velocity $1/\sqrt{2}$ times the stream velocity. This applies equally to the steady value and the fluctuating value of the velocity.

Consider only the fluctuating components in the turbulent stream , because the amplifier filters out all DC wire response components. For two wires at $\pm 45^\circ$ to the stream,

$$v_a = \frac{u + v}{\sqrt{2}} \qquad (67)$$

$$v_b = \frac{u - v}{\sqrt{2}} \qquad (68)$$

Setting $v_a = v_p$, then $v_b = v_p$, equation (66) becomes

$$\left(\frac{\partial \Gamma_{\alpha}}{\partial \alpha}\right)_{\alpha=0} = \left[\frac{\Gamma_{\alpha=\alpha_1} - \Gamma_{\alpha=0}}{\alpha_1 - 0}\right] = (2\pi)^{\frac{1}{2}} \lambda_{\beta}^{\frac{1}{2}} \left\{\frac{\alpha_1 \Gamma_{\alpha_1}}{\left[\beta - \left[1 + \alpha_1^2 (\beta - \Gamma_{\alpha_1}^2)\right]^{\frac{1}{2}}\right]}\right\}$$

$$+ \left\{\frac{\alpha_1 \Gamma_{\alpha_1}}{\left[\beta - \left[1 + \alpha_1^2 (\beta - \Gamma_{\alpha_1}^2)\right]^{\frac{1}{2}}\right]}\right\} \tag{66}$$

A set of eigenfunctions equations can be obtained by setting all quantities at several resistance ratios. For each ratio the above restrictions are overdetermined and the method of two-point at least squares can be used to evaluate the unknowns.

5. Evaluation of Velocity Components.

The foregoing analysis assumed that the velocity was perpendicular to the axis of the wire. Within $10 r_0$ or more from the cylinder, the cooling effect on the wire varies as the cosine of the angle, that is $\cos\theta = \theta_y$. A wire at $10 r_0$ to the upstream stream direction has an average effective velocity $1/\sqrt{2}$ times the normal velocity. This applies equally to the steady value and the fluctuating value of the velocity.

Consider only the fluctuating components in the turbulent stream because the amplifier filters out all DC wire resistance components. The two wires at $\pm 45^{\circ}$ to the stream.

$$v^{\alpha} = \frac{v}{\sqrt{2}} \tag{67}$$

$$v^{\beta} = \frac{v}{\sqrt{2}} \tag{68}$$

Setting $v^{\alpha} = v^{\beta}$, then $v^{\beta} = v^{\alpha}$, equation (66) becomes

$$(2\,i_g)_a^2\left[\frac{M_{sn}^2 - M_n^2}{M_{scn}^2 - M_{sn}^2}\right]_a = 2\,I_a'^2\,(\overline{u^2} + 2\overline{uv} + \overline{v^2}) - \frac{2\sqrt{2}\,\alpha_e\,I_a'\,\bar{I}_a}{\gamma - [1 + \alpha_e(\bar{T}_g - T_e)]}(\overline{ut} + \overline{vt}) + \left\{\frac{\alpha_e\,\bar{I}_a}{\gamma - [1 + \alpha_e(\bar{T}_g - T_e)]}\right\}^2 \overline{t^2} \tag{69}$$

and

$$(2\,i_g)_b^2\left[\frac{M_{sn}^2 - M_n^2}{M_{scn}^2 - M_{sn}^2}\right]_b = 2\,I_b'^2\,(\overline{u^2} - 2\overline{uv} + \overline{v^2}) - \frac{2\sqrt{2}\,\alpha_e\,I_b'\,\bar{I}_b}{\gamma - [1 + \alpha_e(\bar{T}_g - T_e)]}(\overline{ut} - \overline{vt}) + \left\{\frac{\alpha_e\,\bar{I}_b}{\gamma - [1 + \alpha_e(\bar{T}_g - T_e)]}\right\}^2 \overline{t^2} \tag{70}$$

Subtracting (69) from (70):

$$4\left\{i_{sb}^2\left[\frac{M_{sn}^2 - M_n^2}{M_{scn}^2 - M_{sn}^2}\right]_b - i_{sa}^2\left[\frac{M_{sn}^2 - M_n^2}{M_{scn}^2 - M_{sn}^2}\right]_a\right\} =$$

$$2\,(I_b'^2 - I_a'^2)(\overline{u^2} + \overline{v^2}) - 4\,(I_b'^2 + I_a'^2)\,\overline{uv} - \frac{2\sqrt{2}\,\alpha_e}{\gamma - [1 + \alpha_e(\bar{T}_g - T_e)]}(I_b'\,\bar{I}_b - I_a'\,\bar{I}_a)\,\overline{ut} + \frac{2\sqrt{2}\,\alpha_e}{\gamma - [1 + \alpha_e(\bar{T}_g - T_e)]}(I_b'\,\bar{I}_b + I_a'\,\bar{I}_a)\,\overline{vt} + \left\{\frac{\alpha_e}{\gamma - [1 + \alpha_e(\bar{T}_g - T_e)]}\right\}^2(\bar{I}_b^2 - \bar{I}_a^2)\,\overline{t^2} \tag{71}$$

$$+\left\{\frac{2-\left[1+2^{0}(\bar{E}^{2}-\bar{E}^{2})\lambda+1\right]-2}{2^{\frac{1}{2}}\lambda}\right\}\bar{E}_{2}\qquad(11)$$

$$+\frac{2-\left[1+2^{0}(\bar{E}^{2}-\bar{E}^{2})\lambda+1\right]-2}{2^{\frac{1}{2}}\lambda\;\bar{E}^{\frac{1}{2}}}$$

$$-\frac{2-\left[1+2^{0}(\bar{E}^{2}-\bar{E}^{2})\lambda+1\right]-2}{2^{\frac{1}{2}}\lambda\;\bar{E}^{\frac{1}{2}}}$$

$$+\left\{\left[\frac{\bar{E}^{2}-\bar{E}^{2}}{\bar{E}^{2}-\bar{E}^{2}}\right]^{\alpha}-\left[\frac{\bar{E}^{2}-\bar{E}^{2}}{\bar{E}^{2}-\bar{E}^{2}}\right]^{\alpha}\right\}=$$

$$+\left\{\frac{2-\left[1+2^{0}(\bar{E}^{2}-\bar{E}^{2})\lambda+1\right]-2}{2^{\frac{1}{2}}\lambda}\right\}\bar{E}_{1}\qquad(10)$$

$$-\frac{2-\left[1+2^{0}(\bar{E}^{2}-\bar{E}^{2})\lambda+1\right]-2}{2^{\frac{1}{2}}\lambda\;\bar{E}^{\frac{1}{2}}}$$

$$+\left\{\frac{2-\left[1+2^{0}(\bar{E}^{2}-\bar{E}^{2})\lambda+1\right]-2}{2^{\frac{1}{2}}\lambda}\right\}\bar{E}_{2}\qquad(9)$$

$$-\frac{2-\left[1+2^{0}(\bar{E}^{2}-\bar{E}^{2})\lambda+1\right]-2}{2^{\frac{1}{2}}\lambda\;\bar{E}^{\frac{1}{2}}}$$

Fortunately, the two most important quantities of interest in the boundary layer analysis are the dominant terms in this equation. It reduces to

$$(2\,i_g)^2\left[\left(\frac{M_{sn}^2 - M_n^2}{M_{scn}^2 - M_{sn}^2}\right)_b - \left(\frac{M_{sn}^2 - M_n^2}{M_{scn}^2 - M_{sn}^2}\right)_a\right] = -\,8\,I'^2\,\overline{uv} + \frac{2\sqrt{2}\,(\bar{I}_a + \bar{I}_b)\,I'\,\alpha_e}{\gamma - \left[1 + \alpha_e(\bar{T}_g - T_e)\right]}\,\overline{vt} \qquad (72)$$

for two ideally matched wires or a single wire turned successively to the two orientations of $\pm$ 45° to the stream.

Fortunately, the two most important quantities of interest in the boundary layer analysis are the quantities listed in (33) above. In terms of

$$(3\,1^{b}) \qquad \left[\left(\frac{M_1^{con} - M_2^{co}}{M_1^{con} - M_2^{co}}\right)_{\beta} - \left(\frac{M_2^{con} - M_2^{co}}{M_2^{con} - M_2^{co}}\right)_{s}\right] = -\,\frac{1}{\sqrt{2}}\,\frac{\partial \psi}{\partial \eta}$$

$$+ \frac{\beta - \left[1 + \alpha^{2}(\bar{c}^{2} - \bar{c}_{\beta}^{2})\right]}{2\lambda\left[\bar{c}^{2} + \bar{c}_{\beta}^{2}\right]\,\bar{c}^{2}} \frac{\partial \psi}{\partial \eta} \qquad (32)$$

for the slightly modified values of $\bar{c}$ given by (29) corresponding to the two orientations of $\pm\,\Delta\psi_0$ to the stream.

APPENDIX D

EXPERIMENTAL EQUIPMENT AND FACILITIES

(a) Wind Tunnel

The experiments were conducted in a tunnel whose test area has a one foot square cross section. Atmospheric air was drawn through the tunnel by an exhaust fan powered by a one quarter horsepower AC motor. The flow rate through the test section was controlled by a damper in the exhaust line. The maximum velocity attained was approximately twenty-six feet per second. The velocities were measured by a pilot tube probe located on the axis of the tunnel three feet upstream from the test section. A micromanometer was connected to this probe.

The boundary layer was developed over a flat plate which consisted of a twenty-nine inch unheated starting length and a twelve inch heated section. The heating element provided approximately constant heat transfer per unit area. The blunt leading edge of the unheated plate tripped the momentum boundary layer. As shown in Appendix E, the thickness of the momentum and thermal boundary layers at the test station were estimated to be 1.32" and 0.48" respectively.

(b) True RMS Millivoltmeter

An instrument that measures the true root-mean-square voltage of a random input signal was required. There are two commercial meters available which perform this function. They are the Ballantine Laboratories, Inc., model 320 and Flow Corporation, model TRM. The principal difference between them is the manner in which the input signal is averaged. The

APPENDIX B

ROTOR-CURRENT MEASUREMENT AND CALIBRATION

(a) Wire Probes.

The experiments were conducted in a tunnel whose test area had a one foot square cross section. Accordingly six were taken through the tunnel by an exhaust fan powered by a one quarter horsepower motor. The flow rate through the test section was controlled by a damper in the exhaust line. The maximum velocity obtained was approximately twenty-six feet per second. The velocities were measured by a pitot tube probe located on the axis of the tunnel three feet upstream from the test section. A micromanometer was connected to this probe.

The boundary layer was developed over a flat plate which consisted of a twenty-nine inch square piece of plywood mounted vertically in the test section. The leading edge of the plate was rounded to prevent separation. The plate was supported by a rectangular frame which was fastened to the tunnel walls. The plate was positioned so that the leading edge was approximately one inch downstream from the nozzle exit and the plate was parallel to the flow. The boundary layer was investigated at a station which was twenty-four inches from the leading edge of the plate. The thickness of the boundary layer was found to be 1.32" and 0.48" respectively.

(b) Rotor and Drive-Motor.

An instrument that measured the true root-mean-square voltage of a varying input signal was employed. There are two commercial meters available which perform this function. They are the Hallmarking Laboratories, Inc., model 320 rms Determinator, model RMS. The principal difference between them is the manner in which the input signal is averaged. The

model 320 uses an amplifier and a squaring circuit of the segmented type. The model TBM employs a unique design thermal element. The principal characteristics of these instruments are:

Characteristic	Model 320	TBM
meter range (rms volts)	0.0001-320	0.0001-250
frequency response (cycles per second)	15-150,000	2-250,000
linearity over frequency range	± 3%	± 2%
time constant, including meter movements (seconds)	2.25	15
peak factor ≡ ratio of period to pulse width	——	10
crest factor ≡ ratio of peak to rms amplitude	5	——

Due to the presence of many low frequency components in the turbulence velocities being measured, a relatively long averaging period is required for accurate results. The problems encountered with these meters are presented in Section IV.

(c) Probes

Both a single wire and a V-wire probe were used in this series of experiments. Each had tungsten wires of 0.00015" diameter with sensitive lengths of 0.040". These probes are shown in figure 4.

The single wire probe was used to simulate an X-wire probe as noted in the discussion of results. The best results were obtained in this manner. The V-wire probe had a 90° included angle, and the sensitive segments of the wires were located as close as possible to the apex. The

model 320 uses an amplifier and a squaring circuit of the sequence type. The model TBM employs a unique design throughout. The principal characteristics of these instruments are:

Characteristic	Model 320	TBM
meter range (rms volts)	0.0001-320	0.001-150
frequency response (cycles per second)	15-150,000	2-250,000
linearity over frequency range	± 2%	± 1%
time constant, including meter movement (seconds)	2.5	15
peak factor = ratio of pulse to rms value	———	10
crest factor = ratio of peak to rms amplitude	∞	———

due to the presence of many low frequency components in the readings voltmeter using thermocouples, a relatively long settling period is required for accurate results. The procedure recommended with these meters are discussed in Section 12.

(c) Probes

Both a single wire and a V-wire probe were used in this series of experiments. Each had tungsten wires of 0.0003" diameter with sensitive lengths of 0.100". These probes are shown in Figure 6.

The single wire probe was used to visualize an L-wire probe noted in the discussion of results. The best results were obtained by this sensor. The V-wire probe had a 90° included angle, and the sensitive segments of the wires were located as close as possible to the apex. The

resistance of the wires was matched to less than two percent. The problems previously discussed severely limited the use of this probe.

The probes were mounted on a traversing mechanism with a micrometer adjustment to accurately measure the distance from the heated plate. A calibrated index was used to change the angular orientation of the probe.

A carefully constructed X-wire probe correctly oriented to the free stream velocity vector would satisfy the assumptions made in the derivation of equation (72). It would eliminate the principal problems encountered with the V-wire probe - i.e., space resolution and needle resistance. Such a probe was not constructed for this thesis due to fund limitations.

(d) Anemometer Circuits

There are three principal circuits required to transform the wire signal into the data required by equation (72). These are the resistance bridge, square-wave circuit, and amplifier. They are conveniently packaged in the Flow Corporation HWB unit. No other commercially available anemometer equipment meets the requirements for measuring fluctuation quantities.

The bridge circuit provides a method for accurately measuring the wire resistance. This is the fundamental quantity which is sensitive to velocity and temperature fluctuations. The resistance of the wire at any operating condition is calculated from measurements of current ($\bar{I}$), voltage (C_w) and resistance ratio (γ).

The amplifier section boosts the AC components of the voltage across the hot wire to a readable level. It also takes the time derivative of the wire voltage and adds it to a fraction of the wire voltage. This fraction is selected by adjusting the compensation dial to obtain minimum

signal distortion. To properly set the compensation, a square wave is impressed across the bridge circuit and the amplified wire signal is displayed on an oscilloscope. Correct compensation is obtained when the square wave appears linear with a sharp peak at the leading edge. This vertical peak superimposed on a square wave represents the addition of the derivative to the input signal.

Any random input signal to the amplifier may be represented as a Fourier series. The output voltage is therefore a function of frequency. For accurate measurements all of the frequency components should be passed by the amplifier. The HWB has a quoted bandwidth of 2 cps to 100,000 cps. A further error would be introduced by overdriving the amplifier. To prevent this, the attenuator dial was set at '16' which corresponds to 1/16 of the maximum gain.

The square wave circuit provides a reference voltage to the wire for two purposes. First, the square wave is employed to set the amplifier compensation. In addition, it is used to calibrate or normalise the wire voltage that results from stream fluctuations.

One other piece of anemometer equipment, the HWI, was used to a limited extent. It contains a wire current control circuit and a sum-and-difference circuit. It is used in conjunction with the HWB unit and a dual-wire probe. The sum-and-difference of the instantaneous signals from two wires is required to calculate fluctuating velocity components.

(e) Oscilloscope

The output signal of the anemometer amplifier was displayed on an oscilloscope. A Dumont, type 322, dual channel instrument was available in the laboratory. The dual beam presentation will be found particularly useful with an X-wire probe.

signal detection. To properly set the compensation, a square wave is impressed across the bridge circuit and the amplified wave signal is displayed on an oscilloscope. Correct compensation is obtained when the square wave appears flower with a sharp peak at the leading edge. This overshoot peak superimposed on a square wave represents the addition of the derivative to the input signal.

Any random input signal to the oscillator may be considered as a Fourier series. The output voltage is therefore a function of frequency, for accurate measurements all of the frequency components should be passed by the amplifier. The Hewlett was a quoted bandwidth of 3 cps to 150,000 cps. A further error would be introduced by considering the amplifier. By removal this, the attenuator will not act at '1' which corresponds to 1/16 of the maximum gain.

The square wave circuit provides a reference voltage to the wire for the purposes. Then, the square wave is employed in the amplifier correspondence. In addition, it is used to calibrate or normalize the wire voltage that results from micro fluctuations.

The other piece of measuring equipment, the CRO, was used to a limited extent. It consists a wire current control circuit and a push-pull electron circuit. It is easy to manipulation with the CRO unit and a dual-wire probe. The wave-difference of the instantaneous signals from the wires is returned to maintain fluctuating velocity components.

(a) Oscillograph

The output signal of the measuring amplifier was displayed on an oscillograph. A Tektronix, type 122, dual channel instrument was available in the laboratory. The dual beam type will be found particularly useful with an X-wire probe.

APPENDIX E

DATA CALCULATIONS

1. Wire Calibration

Before each wire was calibrated, it was "aged" at a heating current slightly above the maximum operating range. Its velocity response was determined by calibration in the free stream of the tunnel. The wire was oriented perpendicular to the flow and measurements were made of wire current for various resistance ratios. The air velocity was controlled by a damper in the tunnel exhaust line.

A pitot tube with a micromanometer was used to determine the air velocity. A light oil of 0.827 specific gravity filled the manometer tube. All calculations included corrections for atmospheric pressure and temperature in the tunnel; however, since the temperature variations were small, no correction was made for the density changes of the oil. The following equations were employed to calculate velocities in the tunnel:

$$\bar{U} = \sqrt{2gh} = \left[2(g)(h)\ \frac{0.827\,\rho_W}{\rho_A}\right]^{\frac{1}{2}}$$

$$= \left[2(32.2\ \text{ft/sec})\ \frac{h\ \text{inches}}{12\ \text{inches/ft}}\ \frac{0.827 \times 62.2\ \text{lbs/ft}^3}{\rho_A\ \text{lbs/ft}^3}\right]^{\frac{1}{2}}$$

$$\bar{U} = 16.6\left[\frac{h}{\rho_A}\right]^{\frac{1}{2}}$$

where, $\rho_A = \frac{\rho_{\substack{15^\circ c \\ 760mm}}(0.3789)(p\ \text{mm Hg})}{(t^\circ C + 273.2^\circ)} = \frac{(0.07657)(0.3789)(p)}{(t + 273.2)}$

$$\rho_A = \frac{0.02901\ p}{(t + 273.2)}$$

APPENDIX A

DATA CALCULATIONS

1. Pitot Calibration

Before each wind tunnel calibration, it was "zeroed" on a laboratory manometer slightly above the maximum operating range. This velocity pressure was determined by calculation in the form presented at the bottom. The wire was screened perpendicular to the flow and connected into each leg of this manometer for maximum sensitivity reading. The air velocity was controlled by a damper in the tunnel exhaust line.

A plot was made of manometer reading versus air velocity. A light oil of 0.827 density provided fluid for manometer tube. All calculations included corrections for barometric pressure and temperature in the tunnel, however, since the temperature variations were small, no correction was made for the density change of the oil.

The following equations were employed in calculating velocities in the tunnel:

$$V = \sqrt{2gh} = \left[2(g)(D)\ \frac{0.827\ \rho_w}{\rho_a}\right]^{\frac{1}{2}}$$

$$= \left[2(32.2\ \text{ft/sec}^2)\ (\text{in incline/ft})\ \frac{0.827 \times 62.4\ \text{lbm/ft}^3}{\rho_a\ \text{lbm/ft}^3}\right]^{\frac{1}{2}}$$

$$D = 336.6\left[\frac{P}{\rho_a}\right]^{\frac{1}{2}}$$

where, $\rho_a = \frac{P_{barom}(3.1711)(\text{in Hg})}{(t_{oF} + 173.2)^{\circ}R} = \frac{(\text{in Hg})(3.1711)}{(t + 173.2)}$

$$\rho_a = \frac{(t + 173.2)}{0.0390\ t}$$

Typical calculations for two resistance ratios with data taken on 7/3/58 follows:

$$p_A = 762.15 \text{ mm Hg} \; ; \quad t_A = 27.5^\circ \text{ C}$$

$$\rho_A = \frac{(0.02901)(762.15)}{(27.5 + 273.2)} = \frac{22.110}{300.7} = 0.07352 \text{ lbs/ft}^3$$

$$\bar{U} = 16.6 \left[\frac{h}{0.07352}\right]^{\frac{1}{2}} = \frac{16.6}{0.2712} \sqrt{h} = 61.2 \sqrt{h}$$

h in	$\sqrt{h}$ $(\text{in})^{\frac{1}{2}}$	$\bar{U}$ ft/sec	$\sqrt{\bar{U}}$ $(\text{ft/sec})^{\frac{1}{2}}$	I (ma) γ=1.2	γ=1.4	I^2 $(\text{ma})^2$ γ = 1.2	γ = 1.4
0.195	0.442	27.1	5.20	35.06	45.35	1229	2057
0.153	0.391	23.9	4.89	34.48	44.68	1189	1996
0.139	0.373	22.8	4.78	33.90	44.28	1149	1961
0.117	0.342	20.9	4.57	33.80	43.75	1142	1914
0.082	0.286	17.5	4.18	33.18	42.88	1101	1839
0.040	0.200	12.2	3.49	31.35	40.75	983	1661
0.000	0.000	0.0	0.00	23.25	30.32	541	919

This data is plotted in figure 8. The curves follow the general shape predicted by the King equation for hot wires:

$$I^2 = C_1 + C_2 \sqrt{U}$$

2. Determination of $I' \equiv \partial I / \partial U$

The slope of the curve of wire current versus incident velocity (I') is one of the quantities required for the solution of equation 72. Differentiating the King equation, we obtain

$$2 I \cdot \partial I = 0 + C_2 (U)^{\frac{1}{2}} \partial U$$

$$I' \equiv \left(\frac{\partial I}{\partial U}\right)_t = \frac{C_2}{2 I \sqrt{U}}$$

Typical calculations for two Swallowtail returns with data taken on 7/3/52 follow:

$$\text{Ph} = 761.13 \text{ mm Hg} \; ; \; t_K = 23.5^\circ \text{ C}$$

$$\rho_K = \frac{(0.0289)(761.13)}{(23.5 + 273.1)} = \frac{22.010}{320.7} = 0.07313 \text{ lbm/ft}^3$$

$$\bar{U} = 1.3 \left[\frac{0}{0.07313}\right]^{\frac{1}{2}} = \frac{1.3\sqrt{0}}{0.2705} \sqrt{0} = 0 \sqrt{0}$$

θ	$\frac{t_s}{(\cos)^4}$	$\frac{\bar{U}}{\text{ft/sec}}$	$\frac{t_0}{\text{ft/sec}}$	$\frac{1}{\theta_{0.4}}$ (sec) $\gamma=1.5$	$\gamma=1.3$	$\frac{t_s}{(\cos)^4}$ $\gamma=1.4$
0.000	0.000	0.0	0.00	13.23	30.35	344	819
0.040	0.240	12.7	1.48	21.39	49.23	863	1982
0.082	0.284	17.3	4.22	20.18	12.80	1209	1509
0.117	0.342	20.8	4.21	19.80	10.17	1041	1914
0.138	0.313	21.8	4.74	19.60	44.82	1144	1981
0.153	0.301	21.9	4.89	19.45	44.44	1180	1994
0.193	0.442	27.1	5.80	19.04	43.71	1140	2052

Plotted on figure 8. The curves follow the general shape

$$\frac{t_s}{} = c_1 + c_2 \ln$$

3. Determination of γ and $\theta_{0.4}$

The slope of the curve of wave constant versus horizontal velocity (Σ^2 is one of the quantities required for the solution of equation 12. Differentiating the first equation, we obtain

$$\frac{1}{} = c_2 \ln \theta + c_1$$

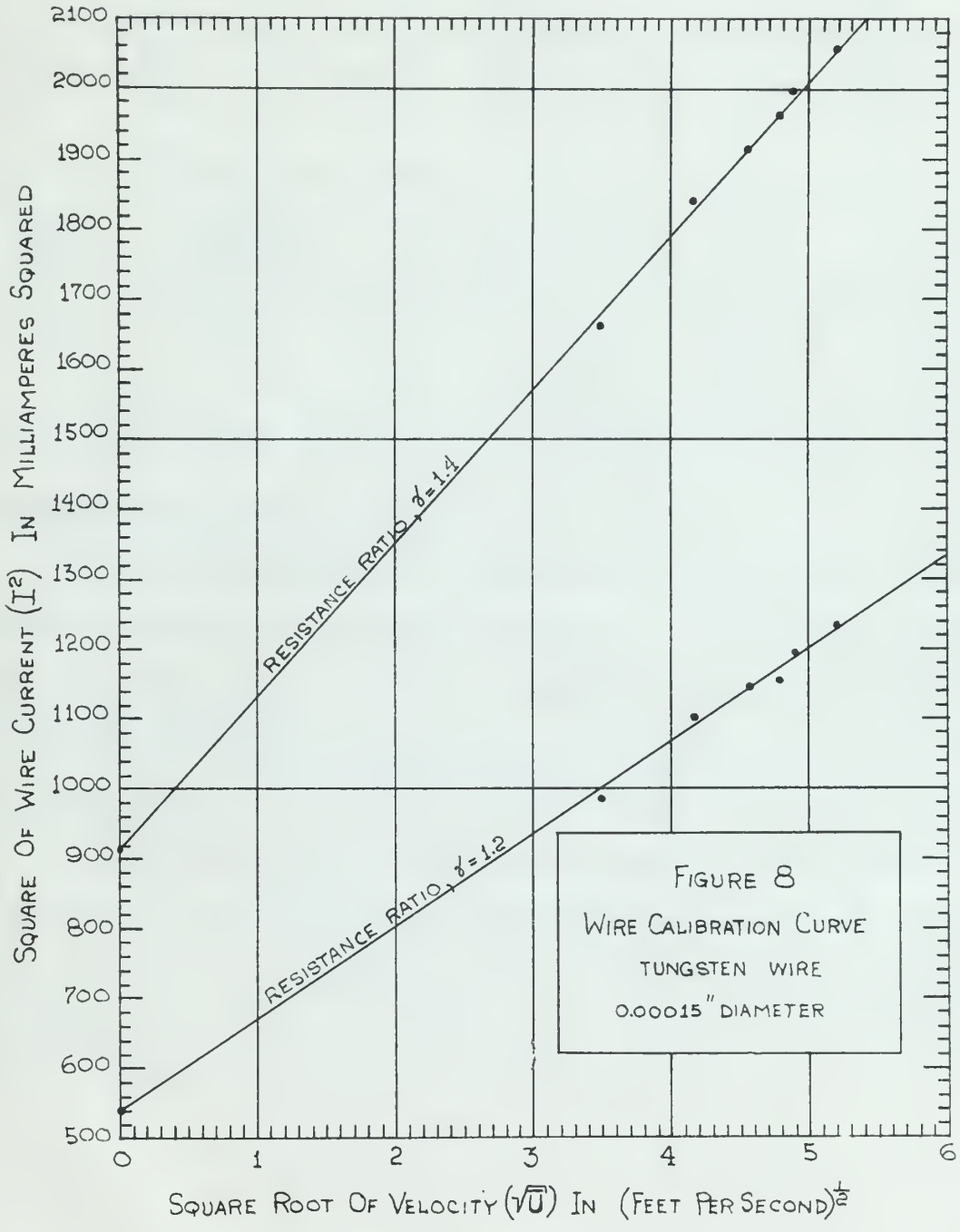

FIGURE 8

WIRE CALIBRATION CURVE

TUNGSTEN WIRE

0.00015" DIAMETER

where C_2 is the slope of the calibration curves obtained in part 1. above. For the free stream velocity chosen for a particular experimental run, the value of $(\sqrt{U})$ is computed and the corresponding current (I) is read from the calibration curve. With these values, the required slope (I') is calculated. Results are shown for a tunnel velocity of twenty-six feet/second.

U ft/sec	$\sqrt{U}$ $(ft/sec)^{\frac{1}{2}}$	γ	C_3 $(ma)^2/ft/sec)^{\frac{1}{2}}$	I ma	I' ma/ft/sec
26.0	5.10	1.2	132.6	34.86	0.1865
		1.4	217.4	45.03	0.2366

3. Amplifier Compensation

As discussed in appendix C, a square wave is employed as a reference voltage to determine the anemometer's response to a fluctuating voltage across the wire. The H-W amplifier compensation is set by observing on an oscilloscope the waveform which results when a square wave is impressed on the wire circuit. An undistorted waveform indicates the proper calibration.

To determine the effect of compensation setting on the voltmeter output, measurements were made in the free stream with the hot wire oriented vertically. The values of M_{an} and M_{scn} were recorded as the compensation was varied.

where C_3 is the slope of the calibration curves obtained in part 1, above. For the true ac/dc values given for a particular experimental run, the ratio of $(\sqrt{V})$ is computed and the corresponding current (I) is read from the calibration curve. With these values, the required slope (I') is calculated. Results are given for a central velocity of 244.0 feet/second.

$\frac{V}{ft/sec}$	$(\frac{ft}{sec})^{\frac{1}{2}}$	γ	$(\mu a)^2/(ft/sec)^{\frac{1}{2}}$	I μa	$\frac{I'}{\mu a/(ft/sec)}$
244.0	5.10	1.2	138.3	34.46	6.1068
		1.4	317.6	49.63	6.2966

3. Amplifier Compensation

As discussed in Appendix C, a square wave is employed as a reference voltage to determine the anemometer's response to a fluctuating voltage across the wire. The dc amplifier compensation is set by observing on an oscilloscope the waveform which results when a square wave is impressed on the wire circuit. An undistorted waveform indicates the proper calibration.

To determine the effect of compensation setting on the voltmeter output, measurements were made in the free stream with the hot wire oriented perpendicularly. The values of E_{dc} and E_{ac} were recorded as the compensation was varied.

Dial Setting	M_{gn} (mv)	M_{gcn} (mv)	M_{gn}^2	M_{gcn}^2	M_n^2	M_g^2	M_c^2	$(\frac{M_g}{M_c})^2$
60	12.8	47.3	164	2230	64	100	2066	0.0484
80	13.3	55.2	176	3040	64	112	2864	0.0391
100	15.6	64.7	242	4170	64	178	3928	0.0454
125	16.2	74.0	262	5460	64	198	5198	0.0381
150	17.2	84.0	296	7050	64	232	6754	0.0344
200	22.2	126	492	15850	64	428	15358	0.0278

This data is plotted in figure 9. The response is approximately linear with no sharp null or peak; hence, proper calibration is difficult. It is estimated that the error introduced in the quantity $(M_g/M_c)^2$ when setting the compensation is of the order of 8.2% when the dial is varied by one dial unit.

4. Square Wave Current

Reference 12 gives the following formula for computing the square current of the HWB:

$$i_s = \frac{3.05}{1 + \frac{(BN)(\gamma)}{400}} = \frac{1220}{400 + (BN)(\gamma)} \cong \frac{1220}{D}$$

where (BN) is the bridge null setting. It is important to maintain the battery supplying this current near its rated voltage.

Test Designation	d_{ca} (cm)	P_{ave} (psi)	P_{max}	M_{ca}	M_c	M_c	$\left(\frac{M_c}{M_c}\right)^2$
80	13.6	412.3	134	3230	84	100	1068	0.0686
80	13.2	13.2	124	3040	64	112	1284	0.0891
100	15.6	04.7	342	4120	64	172	3020	0.0434
122	12.3	74.0	112	2460	60	194	3194	0.0361
130	17.2	34.0	284	7030	64	232	4134	0.0344
200	22.1	122	492	12620	64	420	12320	0.0224

This data is plotted in figure 9. The relationship is approximately linear with no abrupt evil of small beam, plane collapse is evident. It is mentioned that the second intercepted is the quantity D_f^3/D_c^3 when applying the compensation is of the order of 0.25 when the yield is varied by some other means.

4. Buckle Load Capacity

Reference 12 gives the following formula for computing the ultimate strength of the web:

$$\frac{P_u}{P_y} = \frac{1}{1 + \frac{3}{4}\left(\frac{d_w}{t_w}\right)\frac{P_y}{E}} + \frac{1}{\frac{d_w}{t_w} + \left(\frac{d_w}{t_w}\right)\frac{P_y}{E}} \cdot \frac{1}{\frac{P_y}{E}}$$

where (D) is the buckle unit deflection. It is important to maintain the beginning applying this formula when the rated voltage.

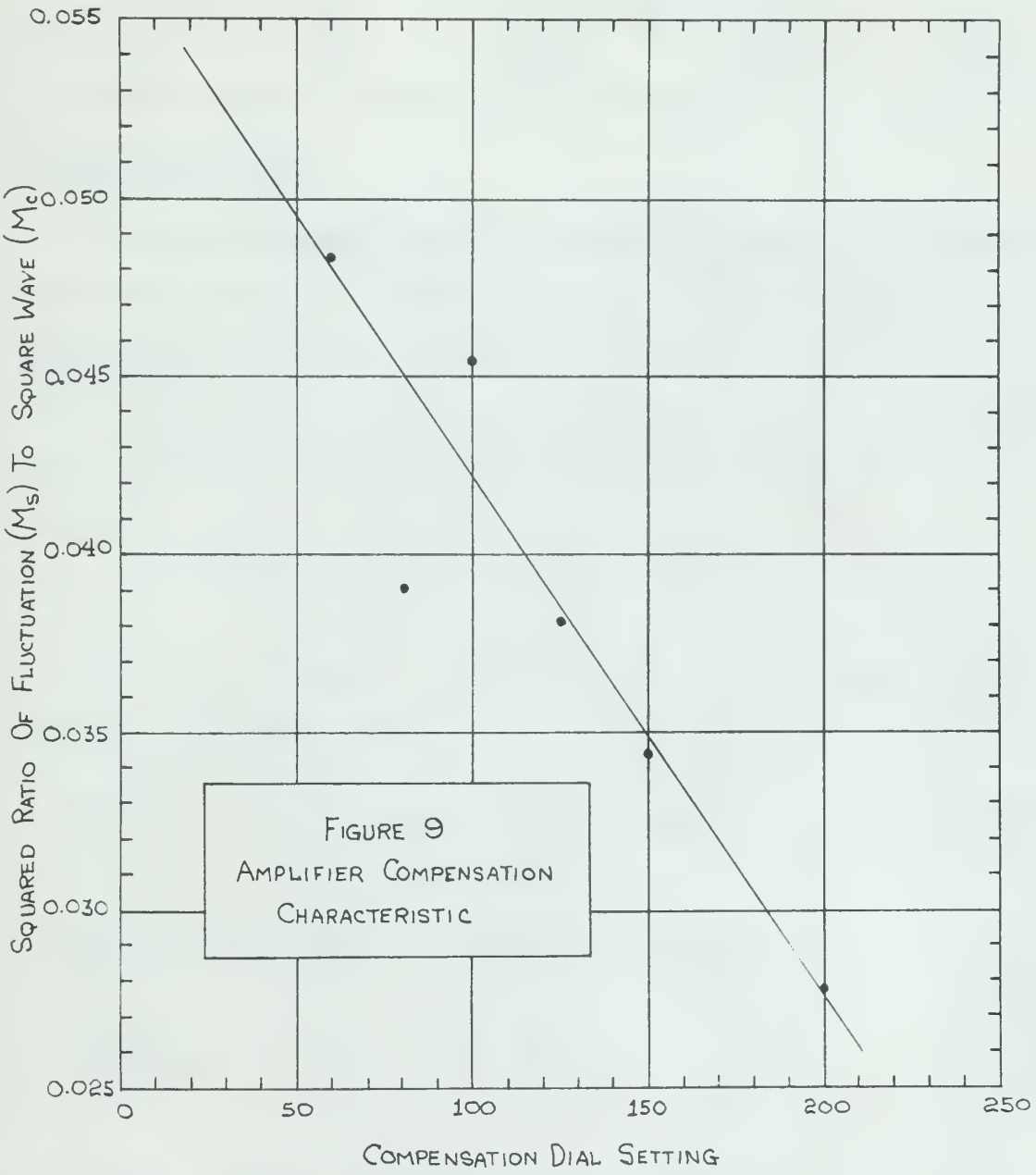

Figure 9
Amplifier Compensation
Characteristic

γ	BN	$(\gamma)(BN)$	D	i_g (ma)
1.2	477	572.4	972.4	1.255
1.4	477	667.8	1067.8	1.142

5. Temperature Profile

The pertinent formula for calculating the difference ($\overline{\Delta T}$) between the temperature (T_g) at a point in the thermal boundary layer and the stream ambient temperature is derived as follows:

$$F(pV) = \frac{I_1^2 R_o \alpha_o}{L}\left(\frac{R}{R-R_g}\right) = \frac{I_2^2 R_o \alpha_o}{L}\left(\frac{R}{R-R_e}\right)$$

$$\text{from which, } \left(\frac{I_1}{I_2}\right)^2 = \frac{R - R_g}{R - R_e} = \frac{T - \bar{T}_g}{T - T_e}$$

where (I_1) is the wire current for a cold plate and (I_2) is that current for the heated plate.

$$\text{Taking } R = R_g\left[1 + \alpha_g(T - \bar{T}_g)\right] \text{ and rearranging, } T = \bar{T}_g + \left(\frac{\gamma-1}{\alpha_g}\right)$$

$$\text{substituting, } \left(\frac{I_1}{I_2}\right)^2 = \frac{\left[(\gamma-1)/\alpha_g\right]}{\left[(\gamma-1)/\alpha_g\right] + (\bar{T}_g - \bar{T}_e)} .$$

$$\text{Rearranging, } \quad (\bar{T}_g - T_e) = \frac{\gamma - 1}{\alpha_g}\left[1 - \left(\frac{I_1}{I_2}\right)^2\right] ;$$

$$\text{taking, } \alpha_g = \frac{\alpha_e}{1 + \alpha_e(\bar{T}_g - T_e)} = \frac{\alpha_e}{1 + \alpha_e(\overline{\Delta T})}$$

λ	Re	$(\delta_T)(Re)$	D	$\frac{A_a}{(Re)}$
1.2	477	572.4	872.4	1.255
1.4	477	667.4	1067.8	1.142

5. Temperature Profile

The pertinent formula for calculating the difference ($\overline{\Delta T}$) between the temperature (T_s^s) at a point in the thermal boundary layer and the stream ambient temperature is derived as follows:

$$(\rho v) = \frac{k}{\frac{1}{2} I_1^2 R^{\alpha} e} \left(\frac{R-R_e}{\delta}\right) = \frac{k}{\frac{1}{2} I_2^2 R^{\alpha} e} \left(\frac{R}{R-R_e}\right)$$

from which, $\left(\frac{I_2^2}{I_1^2}\right) = \frac{R-R_e}{R} = \frac{T-T_e}{T-\overline{T}^s}$

where (I_1^2) is the wire current for a cold plate and (I_2^2) is that current for the heated plate.

Taking $R = R^s\left[1+\alpha^s(\overline{T}-\overline{T}^s)\right]$ and rearranging, $T = \overline{T}^s + \left(\frac{\alpha^s}{\lambda-1}\right)$

substituting, $\left(\frac{I_2^2}{I_1^2}\right) = \frac{\left[(\lambda-1)/\alpha^s\right]}{\left[(\lambda-1)/\alpha^s\right] + (\overline{T}^s-T_e)}$.

Rearranging, $(\overline{T}^s - T_e) = \frac{\alpha^s}{\lambda-1}\left[1-\left(\frac{I_2^2}{I_1^2}\right)\right]$;

taking, $\alpha^s = \frac{1+\alpha^s(\overline{T}^s-T_e)}{\alpha^s} = \frac{1+\alpha^s(\overline{\Delta T})}{\alpha^s}$

and substituting, it can be shown that

$$(T_g - T_e) = \frac{1}{\alpha_e \left[\frac{1}{(\gamma - 1)\left[1 - (I_1/I_2)^2\right]} - 1 \right]} \qquad (73)$$

For an ambient temperature of 24.8° C, the coefficient (α_e) is computed as follows:

$$\alpha_e = \frac{\alpha_o}{1 + \alpha_o(T_e - T_o)} = \frac{0.00454}{1 + 0.00454(24.8^\circ - 20^\circ)} = 0.00444$$

Since the wire is more sensitive to temperature variations at low currents, the data for the temperature profile was taken at a resistance ratio of 1.1. That data and the values computed with equation 73 are shown in the table below and plotted in figure 10.

y (in)	I_1 (ma)	I_2 (ma)	$(\bar{T}_g - T_e)$ (°C)	$\frac{(\bar{T}_g - T_e)}{T_s - T_e}$ (C°)
0.068"	20.91	22.51	3.13°	0.391
0.118"	21.06	24.05	3.78°	0.472
0.168"	22.41	23.42	1.92°	0.240
0.218"	22.75	23.51	1.45°	0.181
0.268"	23.06	23.66	1.13°	0.141
0.368"	23.35	23.74	0.73°	0.091
0.468"	23.92	23.85	-0.14°	-0.018

The normalized temperature profile is plotted in figure 2 of Section III.

The experimental data points are plotted in figure 2 of section III.

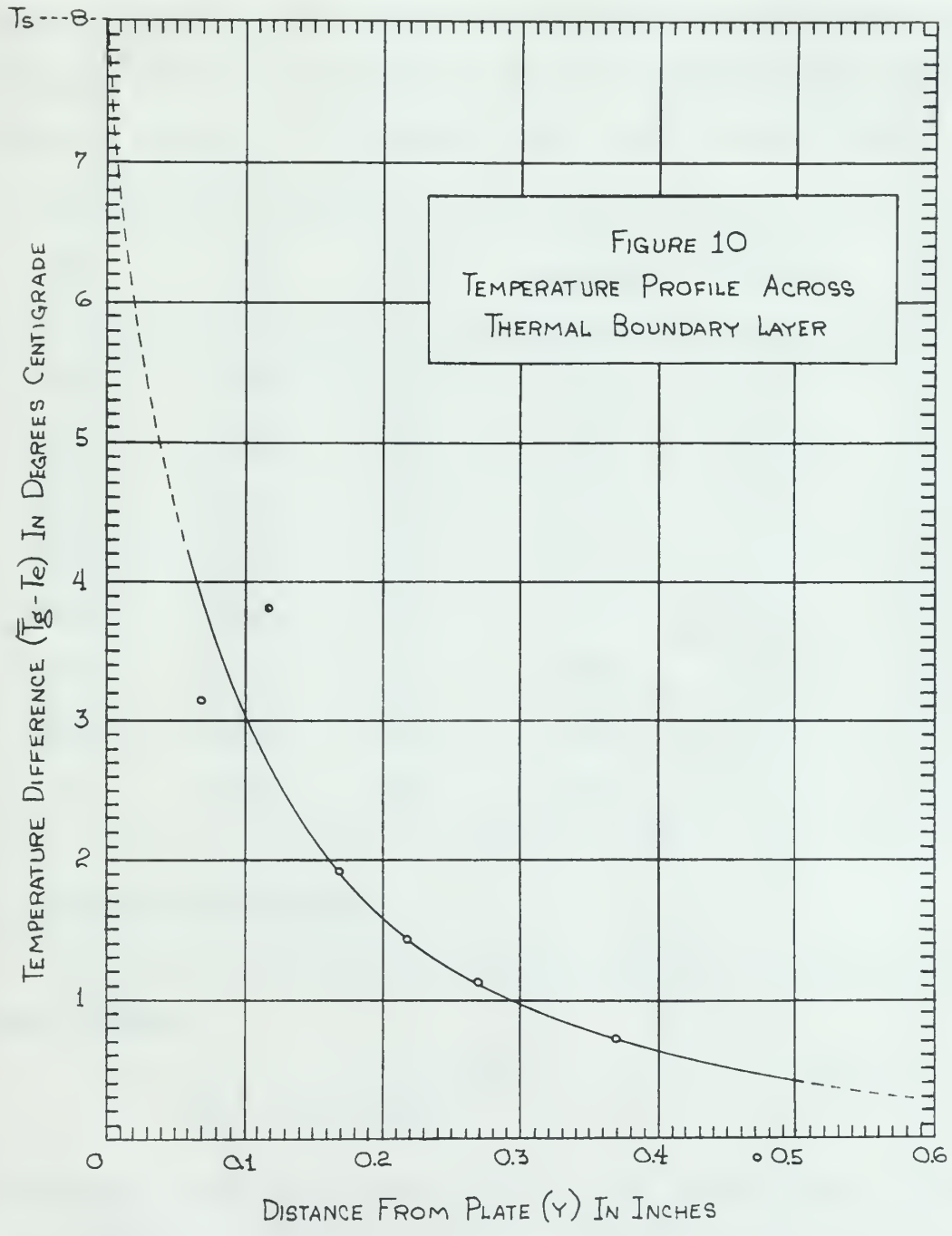

Figure 10
Temperature Profile Across
Thermal Boundary Layer

6. Velocity Profile

The velocity profile across the momentum boundary layer is obtained with the plate cold and the wire oriented vertically. The values of current recorded are then used as arguments to enter figure 8 and determine the velocity. The data and results are shown below together with a plot of the profile in figure 11. The normalized plot appears in the RESULTS.

y (in)	i (ma)	i^2 $(ma)^2$	$\sqrt{\bar{U}}$ $(ft/sec)^{\frac{1}{2}}$	$\bar{U}$ (ft/sec)	$\frac{\bar{U}}{U_\infty}$
0.068"	44.00	1936	4.63	21.44	0.758
0.118"	44.35	1967	4.78	22.85	0.807
0.168"	44.48	1978	4.82	23.23	0.821
0.218"	44.68	1996	4.95	24.50	0.866
0.268"	44.78	2005	4.99	24.90	0.880
0.368"	44.98	2023	5.04	25.40	0.898
0.468"	45.12	2036	5.10	26.01	0.920
℄	45.70	2088	5.32	28.30	1.000

7. Boundary Layer Thickness

The following equation may be used to predict the momentum boundary layer thickness,

$$\delta_m = 0.37x\left(\frac{V_\infty x}{\nu}\right)^{-1/5}$$

Considering a point twenty-nine inches from the leading edge of the plate and a free stream velocity of twenty-six feet per second, the thickness will be,

6. Velocity Profile

The velocity profile across the momentum boundary layer is obtained with the plate cold and the stys unheated vertically. The values of current recorded are then used as explained in notes figure 9 and determine the velocity. The data and results are shown below together with a plot of the profile in figure 11. The boundaries plot otherwise in the margin.

y (in)	x (in)	Σ_E (in)	$\sqrt{\frac{E}{R}}$ (ft/sec)	$\bar{u}$ (ft/sec)	$\frac{\bar{u}}{u_\infty}$
0.088"	44.01	1934	4.83	21.40	0.758
0.112"	44.33	1932	4.78	22.03	0.802
0.138"	44.46	1934	4.82	23.13	0.821
0.212"	44.80	1944	4.93	24.50	0.869
0.248"	44.74	1946	4.89	24.80	0.880
0.328"	44.90	1951	5.04	25.80	0.914
0.468"	45.15	1954	5.10	26.45	0.938
∞	45.10	1948	5.11	26.30	1.000

7. Momentum Layer Thickness

The following equation may be used to measure the momentum boundary layer thickness,

$$\frac{\delta}{x} = 0.378 \left(\frac{\nu}{u_\infty x}\right)^{1/5}$$

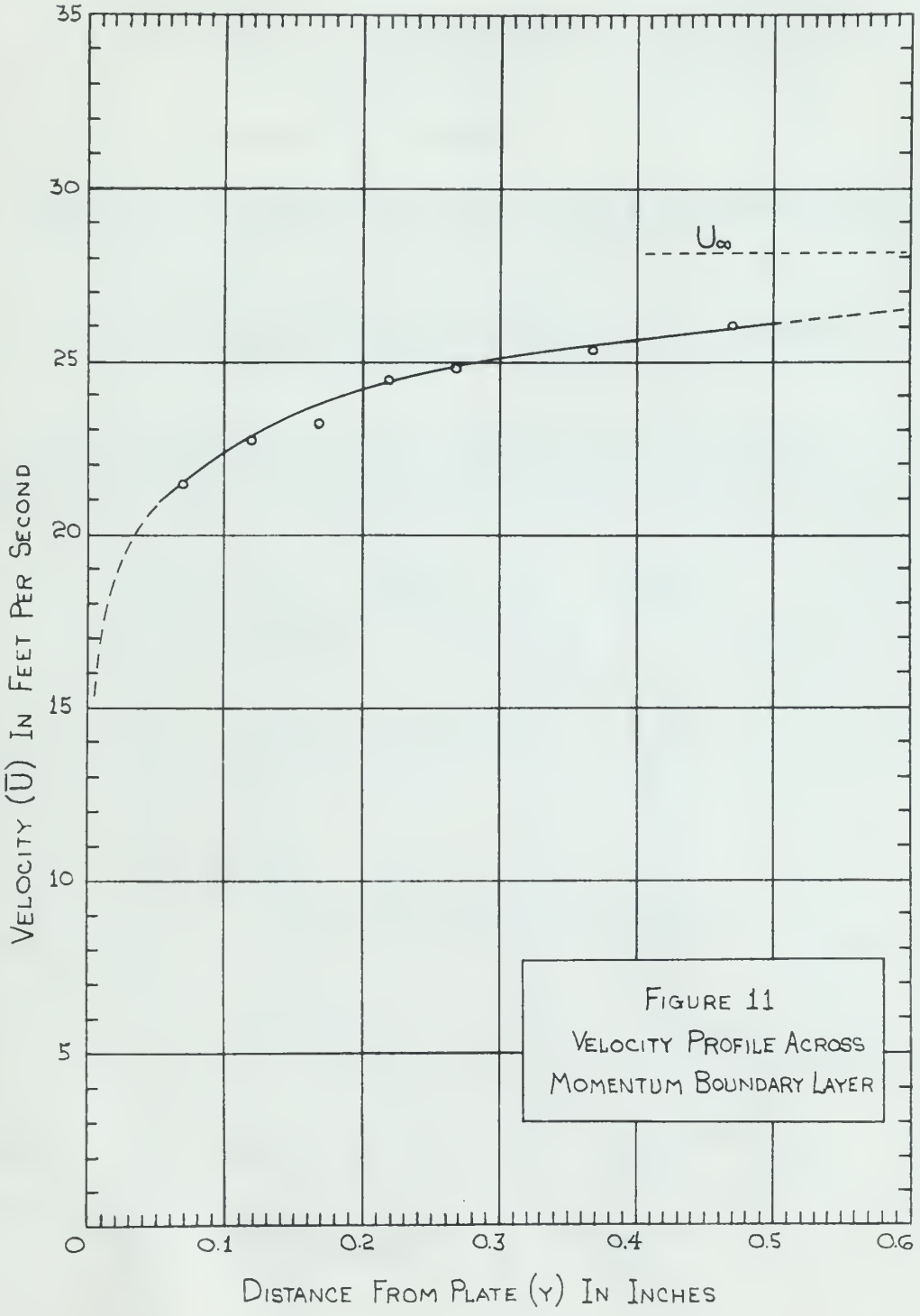

Figure 11
Velocity Profile Across
Momentum Boundary Layer

$$V_\infty = (26 \text{ ft/sec})(3600 \text{ sec/hr}) = 9.36 \times 10^4 \text{ ft/hr.}$$

$$\rho = \frac{(0.02901)(p \text{ mm Hg})}{(t^{\circ}C + 273.2^{\circ})} = \frac{(0.02901)(767.05)}{(298.0)} = 0.0747 \text{ lbs/ft}^3$$

$$\nu = \frac{\mu}{\rho} = \frac{0.460 \text{ lbs/ft-hr}}{0.0747 \text{ lbs/ft}^3} = 6.16 \frac{\text{ft}^2}{\text{hr}}$$

$$x = 29 \text{ inches} = 2.42 \text{ ft.}$$

$$\text{then } \delta_m = (0.37)(29 \text{ inches}) \left[\frac{(9.36 \times 10^4 \text{ ft/hr})(2.42 \text{ ft})}{(6.16 \text{ ft}^2/\text{hr})}\right]^{-1/5}$$

$$\delta_m = \frac{(10.73)}{(3.68 \times 10^4)^{1/5}} = \frac{(10.73)}{(8.13)} = 1.32 \text{ inches}$$

This thermal boundary layer thickness may be calculated in a similar manner employing the following equation taken from reference 14,

$$\delta_t = K_g \left(\frac{V_\infty x}{\nu}\right)^{\frac{35b-36}{5(15-7b)}} \left(\frac{C_p \mu}{k}\right)^{\frac{7(c-1)}{15-7b}} (x)$$

$$\text{where, } K_g = \left[\frac{0.37^{1/7} \times 72K}{7}\right]^{\frac{7}{15-7b}}$$

$$K = 0.0167; \quad b = 4/5; \quad c = 1/3$$

$$\text{substituting, } K_g = \left[\frac{(0.37^{1/7})(72)(0.0167)}{7}\right]^{\frac{7}{15-5.6}} = 0.243$$

$$N_{pr} = \frac{C_p \mu}{k} = 0.71 \text{ and } x = 10 \text{ inches}$$

$$\text{then, } \delta_t = 0.243 \, (3.68 \times 10^4)^{-0.1701} \, (0.71)^{-0.497} \, (10)$$

$$\delta_t = \frac{(2.43)}{(5.96)(0.844)} = 0.483 \text{ inches}$$

$$V_{ma} = (26 \text{ ft/sec})(3600 \text{ sec/hr}) = 9.36 \times 10^4 \text{ ft/hr.}$$

$$\rho = \frac{(0.625)(0.00 \text{ lbm})}{(\text{ft}^3 + 173.2^\circ)} = \frac{(0.0290)(7.12 \text{ lbm})}{(230.0)} = 0.0047 \text{ lbm/ft}^3$$

$$\gamma = \frac{\mu}{\rho} = \frac{0.0\text{xx lbm/ft-hr}}{0.0747 \text{ lbm/ft}^3} = 0.10 \frac{\text{ft}^2}{\text{hr}}$$

$$x = 29 \text{ inches} = 2.42 \text{ ft.}$$

$$\text{then } \delta_m = (0.37)(29 \text{ inches}) \left[\frac{(9.29 \times 10^4 \text{ ft/hr})(2.42 \text{ ft})}{(0.10 \text{ ft}^2/\text{hr})} \right]^{-1/2}$$

$$\delta_m = \frac{(10.2)}{(3.04 \times 10^4)^{1/2}} = \frac{(10.2)}{(0.12)} = 1.32 \text{ inches}$$

Onto thermal boundary layer thickness may be calculated in a similar manner employing the following equation taken from reference 14.

$$\delta_t = N_{Pr}^{-\frac{1}{3}} \left(\frac{\mu}{\rho V} \right) \left(\frac{x}{x} \right)^{\frac{1}{2}} \frac{\Gamma(\epsilon-1)}{\Gamma(\epsilon-\frac{1}{2})} \frac{2\beta-2\epsilon}{3\epsilon-2\epsilon}$$

where, $N_{Pr} = \left[\frac{0.72^{1/2} + (2\beta}{2} \right]^{\frac{1}{1-2\epsilon}}$

$\epsilon = 0.0207$; $\beta = 0.5$; $c = 1/3$

substituting, $x^0 = \left[\frac{(0.37)^{1/2}}{2} (72)(0.0247) \right]^{\frac{2}{1.5-1.0}} = 0.243$

$$\beta_{Pr} = \frac{\mu}{\rho V} = 0.71 \text{ and } x = 10 \text{ inches}$$

then, $\delta_t = 0.243 \ (3.83 \times 10^4)^{-0.1201} \ (0.71)^{-0.497} \ (10)$

$$\delta_t = \frac{(2.43)}{(5.96)(0.844)} = 0.483 \text{ inches}$$

8. $\overline{uv}$ Correlation in "Cold" Momentum Boundary Layer

In the cold plate condition, equation 7 may be used to calculate the quantity $\overline{uv}$.

$$\overline{uv} = -\frac{i_s^2}{2(I')^2}\left[\left(\frac{M_{sn}^2 - M_n^2}{M_{scn}^2 - M_{sn}^2}\right)_b - \left(\frac{M_{sn}^2 - M_n^2}{M_{scn}^2 - M_{sn}^2}\right)_a\right]$$

Data was taken at two resistance ratios and averaged. The values of (I') were taken from section (b) of this appendix, while i_s was calculated for a bridge null setting of 483 by the method of section 4. The remaining data is shown in tabular form together with the results obtained, which are plotted in the RESULTS.

						averaged values	
		γ = 1.2					
y (in)	$(M_{sn})_a$ (mv)	$(M_{scn})_a$ (mv)	(M_n) (mv)	$(M_{sn})_b$ (mv)	$(M_{scn})_b$ (mv)	$\overline{uv}$ $(ft/sec)^2$	$\frac{\overline{uv}_2}{U_\infty}$
0.068	24.2	61.2	7.50	31.0	62.8	-2.75	-0.00407
0.118	23.4	61.3	"	29.2	63.3	-2.48	-0.00367
0.168	21.8	61.2	"	27.3	62.6	-2.25	-0.00333
0.218	20.8	60.7	"	25.7	61.0	-1.82	-0.00269
0.268	19.4	60.2	"	24.8	61.5	-1.40	-0.00207
0.368	19.1	59.7	"	23.3	62.4	-1.29	-0.00191
0.468	17.0	59.0	"	19.6	61.8	-0.929	-0.00137
		γ = 1.4					
0.068	60.9	128.0	7.45	79.5	137.0		
0.118	59.0	128.5	"	73.4	126.5		
0.168	53.5	125.6	"	72.5	131.0		
0.218	50.3	124.0	"	66.3	129.5		
0.268	47.8	123.0	"	60.2	130.5		
0.368	45.5	122.5	"	60.3	127.0		
0.468	40.2	122.3	"	54.5	124.0		

6. Correlation in "Void" Detector Boundary Layer

In the void plate condition, equation 7 may be used to calculate the quantity $\overline{uv}$.

$$\overline{uv} = -\frac{\mu_c}{2(I')^2}\left[\left(\frac{R_{Ba}^2 - R_B^2}{R_{Ba}^2 - R_{Bn}^2}\right)^2 - \left(\frac{R_{Ba}^2 - R_B^2}{R_{Ba}^2 - R_{Bn}^2}\right)^2\right]_a$$

Data was taken at two resistance ratios and averaged. The values of (I') were taken from section (b) of this appendix, while i_o was calculated for a bridge null setting of A80 by the method of section A. The resulting data is shown in tabular form together with the results obtained, when are plotted in the RESULTS.

$\gamma = 1.2$ -averaged values

y (in)	$(M_{uncr})_a$ (mv)	$(M_{uncr})_a$ (mv)	$(M_{Bn})_b$ (mv)	$(M_{Bn})_b$ (mv)	$\overline{uv}$ $(in/sec)^2$	$\frac{\overline{uv}}{U_{\infty}^2}$
0.088	84.2	81.2	7.50	32.0	62.8	-2.75	-0.00407
0.110	23.4	81.2	"	29.2	63.3	-2.46	-0.00367
0.132	21.8	81.2	"	27.3	63.4	-2.25	-0.00333
0.154	20.8	80.7	"	25.7	61.0	-1.82	-0.00269
0.198	19.4	80.2	"	24.8	61.3	-1.46	-0.00207
0.242	18.1	79.7	"	23.2	62.4	-1.16	-0.00171
0.464	17.0	79.0	"	22.6	61.6	-0.939	-0.00137

$\gamma = 1.4$

0.088	60.9	128.0	7.45	73.5	137.6	
0.110	59.0	128.3	"	73.4	126.5	
0.132	53.5	127.6	"	72.3	131.0	
0.154	50.3	124.0	"	66.3	129.5	
0.198	47.8	123.0	"	60.2	130.3	
0.242	43.5	122.5	"	60.3	127.0	
0.464	40.2	122.3	"	54.5	124.0	

9. $\overline{uv}$ and $\overline{vt}$ Correlations in Thermal Boundary Layer

On the hot plate condition, equation 72 may be used to calculate the quantities $\overline{uv}$ and $\overline{vt}$. Rearranged,

$$\overline{uv} = \frac{\sqrt{2}\,(I_a + I_b)}{4\,I'}\left[\frac{\alpha_e}{\gamma - [1 + \alpha_e(\overline{T}_g - T_e)]}\right] = \frac{i_s^2}{2(I')^2}\left[\left(\frac{M_{sn}^2 - M_n^2}{M_{scn}^2 - M_{sn}^2}\right)_b - \left(\frac{M_{sn}^2 - M_n^2}{M_{scn}^2 - M_{sn}^2}\right)_a\right]$$

Data was taken at two resistance ratios as for the previous calculations. Great difficulty was experienced in obtaining reasonable results because of the scattering of the data. To reduce the random errors present the data was plotted in figure 12 through 14, and faired into smooth curves. The remainder of the calculations were carried out with the smoothed data. The raw data, the faired data and the final results are tabulated below. Normalized curves of the results appear in figures 1 and 3.

Raw Data

$\gamma = 1.2$

y (in.)	$4I_a$ (ma)	$4I_b$ (ma)	M_n (mv)	$(M_{sn})_a$ (mv)	$(M_{sn})_b$ (mv)	$(M_{scn})_a$ (mv)	$(M_{scn})_b$ (mv)
0.068	121.0	127.8	7.5	41.7	60.1	61.7	76.5
0.118	121.1	129.9	"	41.2	50.2	61.0	70.2
0.168	125.0	132.2	"	34.3	39.9	58.7	62.6
0.218	126.1	132.3	"	28.1	33.5	56.5	53.7
0.268	128.0	131.8	"	25.1	29.5	53.7	57.5
0.368	128.8	132.9	"	19.7	24.4	52.2	53.5
0.468	130.1	132.8	"	17.7	21.9	52.2	53.0

9. $\overline{uv}$ and $\overline{vt}$ Correlations in Thermal Boundary Layer

On the hot plate condition, equation 7 may be used to calculate the quantities $\overline{uv}$ and $\overline{vt}$. Rearranged,

$$\overline{uv} = \frac{\nu^2}{4} \frac{(I_a + I_b)}{\left[\gamma - \left[1 + \frac{\gamma^2}{12}(K_{en}^2 - K_{en}^2)\right]^2\right]} \frac{\gamma^2}{12}(I^2) \left[\left(\frac{K_{en}^2 - K_{en}^2}{K_{en}^2 - K_{en}^2}\right) - \left(\frac{K_{en}^2 - K_{en}^2}{K_{en}^2 - K_{en}^2}\right)\right]$$

Data was taken at two resistance ratios as for the previous calculations. Great difficulty was experienced in obtaining reasonable results because of the smoothing of the data. To remove the random errors present the data was plotted in figure 13 through 24, and faired into smooth curves. The results of the calculations were carried out with the smoothed data. The raw data, the faired data and the final results are tabulated below. Normalized curves of the results appear in figures 1 and 3.

Raw Data

$\gamma = 1.2$

y (in.)	Δt_a (sec)	Δt_b (sec)	M_{en} (cm)	$(M_{en})_a$ (cm)	$(M_{en})_b$ (cm)	$(M_{con})_a$ (cm)	$(M_{con})_b$ (cm)
0.064	121.0	127.8	7.5	41.7	69.1	83.7	76.5
0.110	121.1	129.9	"	41.2	50.2	81.0	70.2
0.164	125.0	132.2	"	34.3	30.9	38.7	62.6
0.214	126.1	132.3	"	28.1	22.5	56.2	53.7
0.266	128.0	131.8	"	23.1	18.3	35.7	57.5
0.318	128.6	132.3	"	19.7	24.4	31.4	53.5
0.461	130.1	132.8	"	17.7	11.8	32.2	53.0

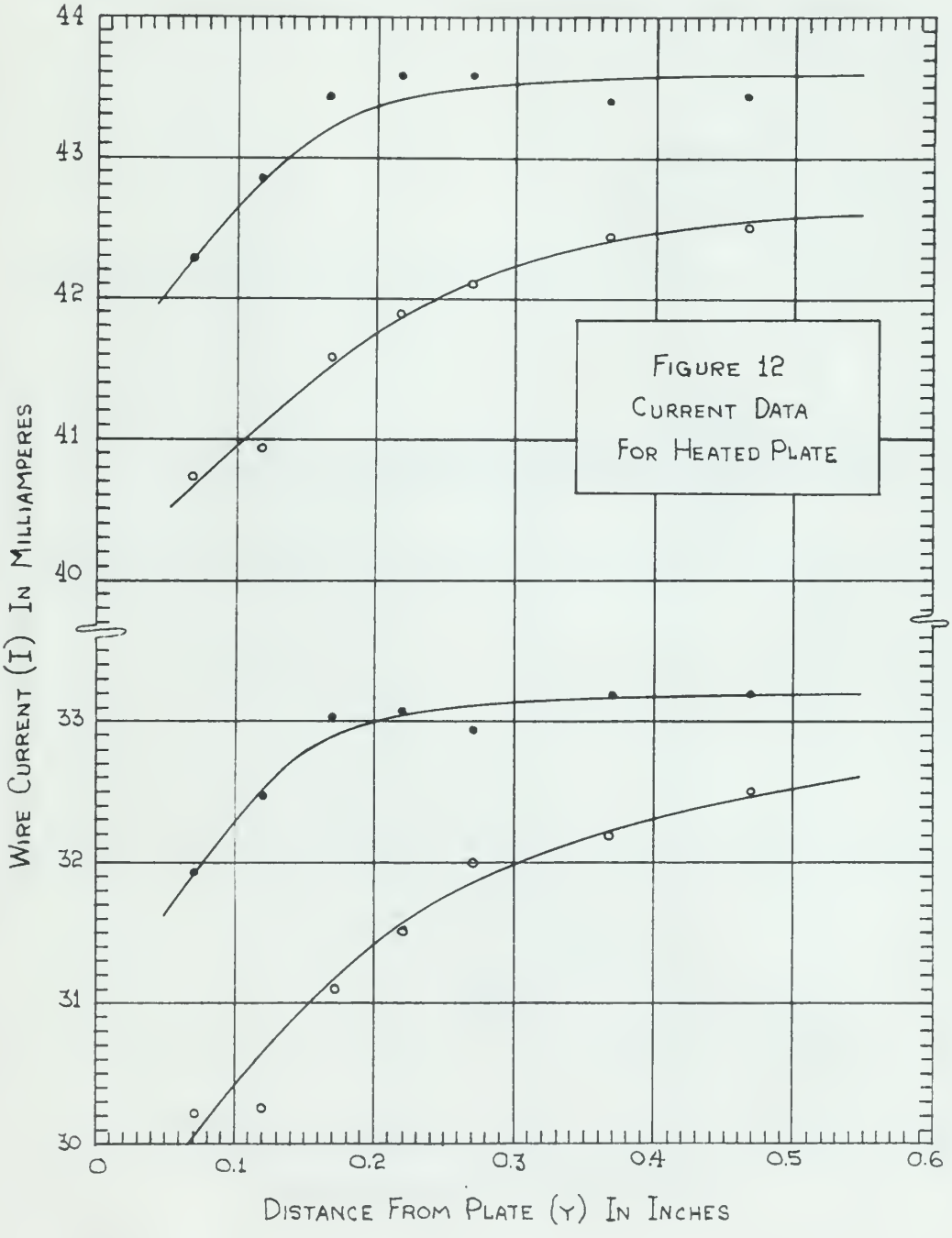
44
43
42
41
40
33
32
31
30
0
0.1
0.2
0.3
0.4
0.5
0.6
Wire Current (I) In Milliamperes
Distance From Plate (Y) In Inches
Figure 12
Current Data
For Heated Plate

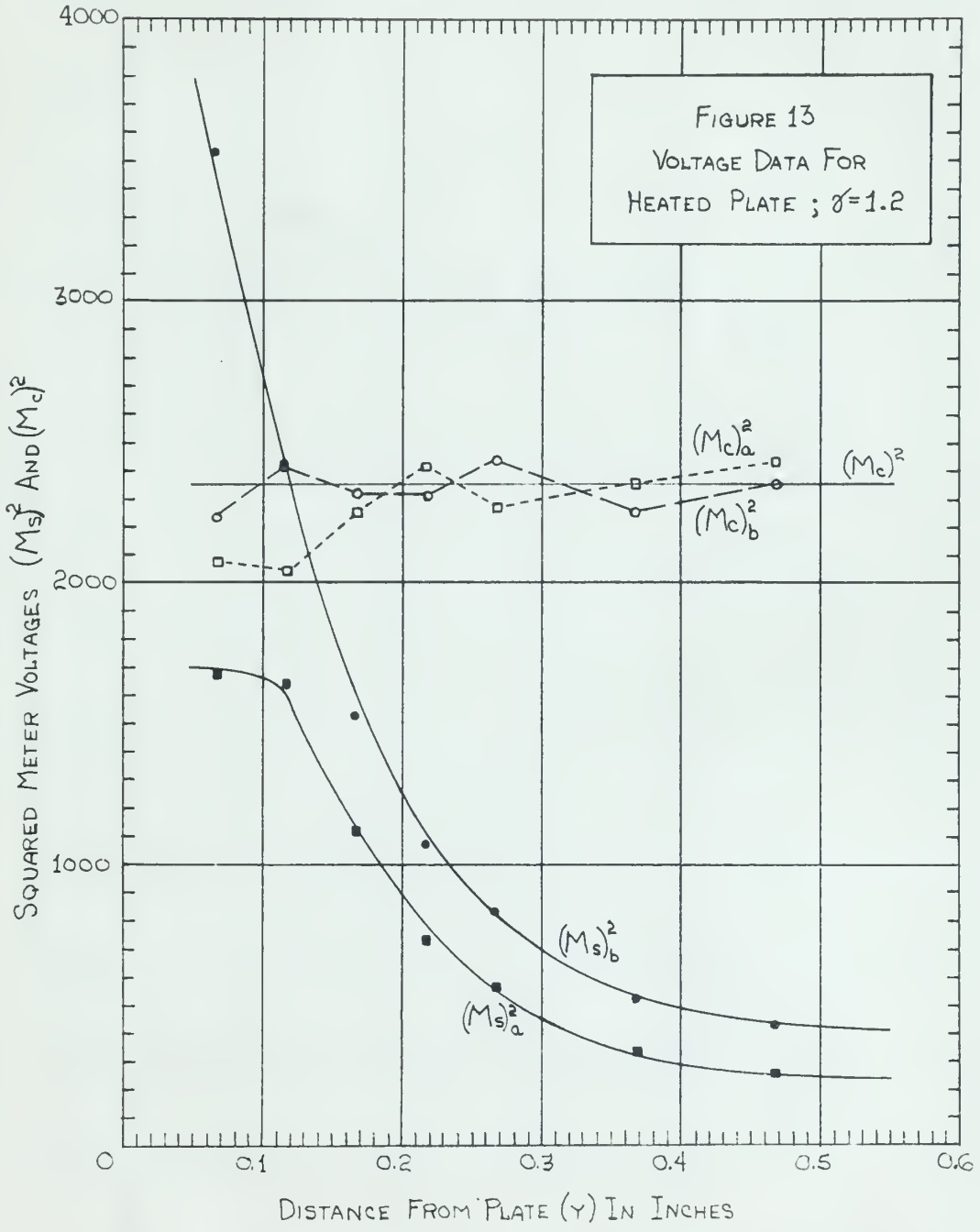
FIGURE 13
VOLTAGE DATA FOR
HEATED PLATE ; γ=1.2
SQUARED METER VOLTAGES $(M_s)^2$ AND $(M_c)^2$
DISTANCE FROM PLATE (Y) IN INCHES
4000
3000
2000
1000
0
0.1
0.2
0.3
0.4
0.5
0.6
$(M_c)^2_a$
$(M_c)^2$
$(M_c)^2_b$
$(M_s)^2_b$
$(M_s)^2_a$

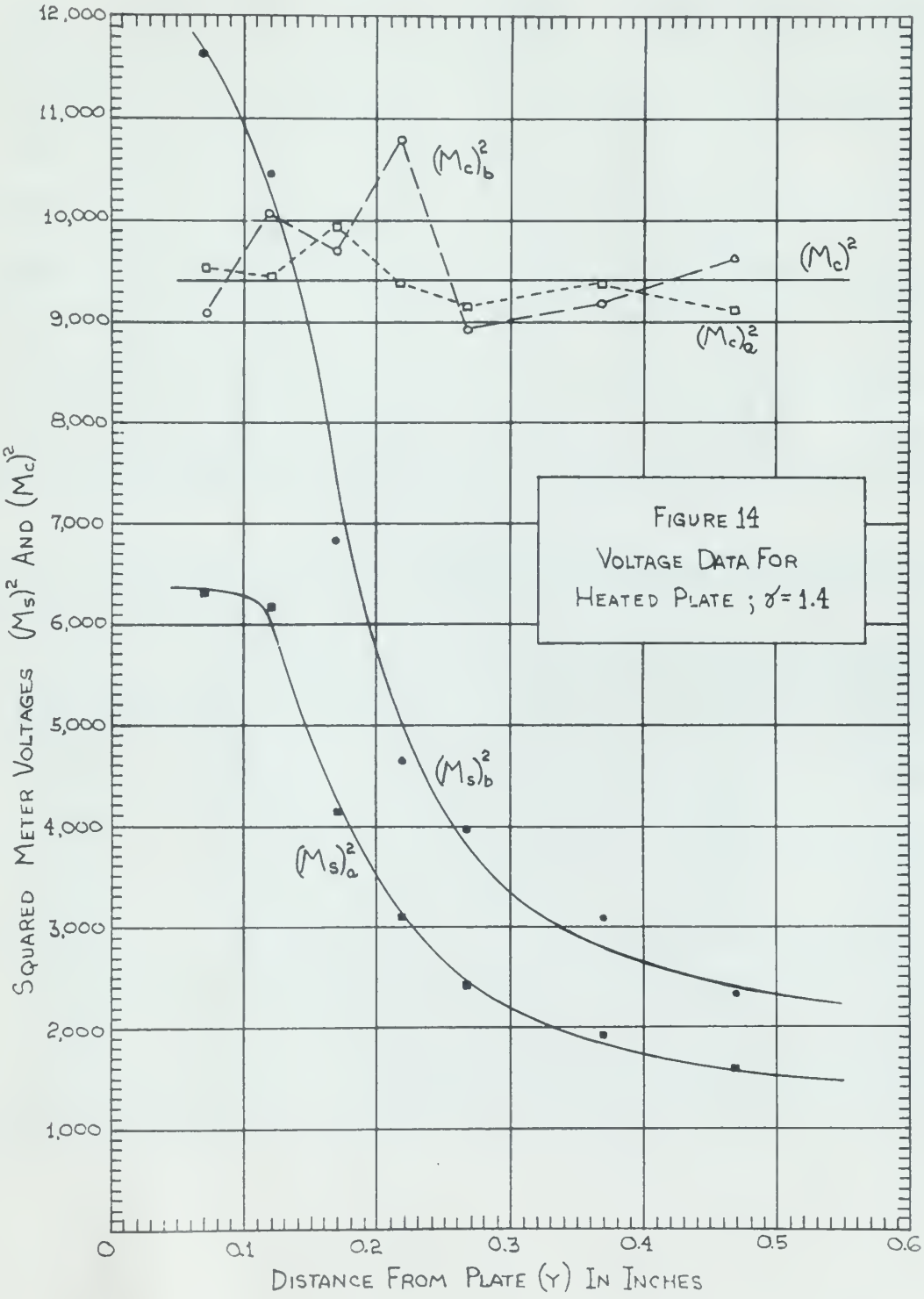

Figure 14
Voltage Data For
Heated Plate ; $\gamma = 1.4$

Raw Data, con.

$\gamma = 1.4$

y (in)	$4I_a$ (ma)	$4I_b$ (ma)	M_n (mv)	$(M_{sn})_a$ (mv)	$(M_{sn})_b$ (mv)	$(M_{scn})_a$ (mv)	$(M_{scn})_b$ (mv)
0.068	163.0	169.2	7.5	79.7	108.0	126.0	144.0
0.118	163.8	171.4	"	78.5	102.5	125.0	143.5
0.168	166.3	173.3	"	64.7	83.1	119.0	129.0
0.218	167.7	174.3	"	56.0	68.6	112.0	124.5
0.268	168.5	174.3	"	49.8	63.6	108.0	114.0
0.368	169.8	173.6	"	44.5	56.0	106.5	111.0
0.468	170.0	173.7	"	41.0	49.3	104.0	110.0

Faired Data

$\gamma = 1.2$

y (in)	I_a (ma)	I_b (ma)	$(M_s)_a^2$ $(mv)^2$	$(M_s)_b^2$ $(mv)^2$	$(M_c)^2$ $(mv)^2$
0.068	30.01	31.93	1690	3520	2350
0.118	30.65	32.51	1620	2410	"
0.168	31.18	32.89	1130	1600	"
0.218	31.60	33.06	770	1100	"
0.268	31.88	33.13	530	810	"
0.368	32.23	33.19	330	550	"
0.468	32.47	33.20	240	440	"

Raw Data, cont.

γ = 1.4

γ (in)	ΔI^a (ma)	ΔI^b (ma)	M_n (mv)	$(M_{an})_a$ (mv)	$(M_{an})_b$ (mv)	$(M_{ecn})_a$ (mv)	$(M_{ecn})_b$ (mv)
0.068	163.0	169.2	7.5	79.7	108.0	126.0	144.0
0.118	163.8	171.4	"	78.5	102.5	125.0	143.5
0.168	166.3	173.3	"	64.7	83.1	119.0	129.0
0.218	167.7	174.3	"	56.0	68.6	112.0	124.5
0.268	168.5	174.3	"	49.5	63.6	109.0	114.0
0.368	169.8	173.6	"	44.5	55.0	106.5	111.0
0.468	170.0	173.7	"	41.0	49.3	104.0	110.0

Paired Data

γ = 1.2

γ (in)	I^a (ma)	I^b (ma)	$(M_a)^2_a$ (mv)^2	$(M_a)^2_b$ (mv)^2	$(M_c)^2$ (mv)^2
0.068	30.01	31.93	1090	3520	2350
0.118	30.65	32.51	1620	2410	"
0.168	31.16	32.89	1130	1900	"
0.218	31.60	33.06	770	1100	"
0.268	31.85	33.13	530	810	"
0.368	32.23	33.19	330	550	"
0.468	32.47	33.20	240	440	"

Faired Data, con.

$\gamma = 1.4$

y (in)	I_a (ma)	I_b (ma)	$(M_s)^2_a$ $(mv)^2$	$(M_s)^2_b$ $(mv)^2$	$(M_c)^2$ $(mv)^2$
0.068	40.87	42.30	6320	11650	9400
0.118	41.13	42.81	6040	10250	"
0.168	41.55	43.22	4190	7380	"
0.218	41.89	43.42	3130	5000	"
0.268	42.10	43.50	2470	3840	"
0.368	42.41	43.56	1830	2790	"
0.468	42.56	43.58	1600	2400	"

Results

y (in)	$\overline{uv}$ $(ft/sec)^2$	$\frac{\overline{uv}}{U_\infty^2}$	$\overline{vt}$ $(ft\,^oC/sec)$	$\frac{\overline{vt}}{U_\infty(T_s-T_e)}$
0.068	+4.69	+0.00694	+7.96	+0.0383
0.118	-2.74	- 0.00405	+1.74	+0.00837
0.168	-3.35	-0.00496	+0.421	+0.00202
0.218	-1.41	-0.00209	+0.633	+0.00304
0.268	-0.641	-0.00095	+0.737	+0.00354
0.368	-0.205	-0.00030	+0.686	+0.00330
0.468	+0.002	+0.00000	+0.693	+0.00333

Table No. 19, cont.

γ = 1.4

γ (in)	I_a (mm)	I_b (mm)	$(M_s)^2_{uv}$	$(M_s)^2_{uv}$	$(M_c)^2_{uv}$
0.068	40.87	42.30	8320	11850	9400
0.118	41.13	42.81	6040	10250	"
0.168	41.55	43.22	4190	7380	"
0.218	41.29	43.42	3130	5600	"
0.268	42.10	43.50	2470	3640	"
0.368	42.41	43.56	1430	2790	"
0.468	42.56	43.58	1600	2400	"

Results

γ (in)	$\overline{uv}$ (ft/sec)^2	U^2_{∞}	$\overline{vt}$ (ft°C/sec)	$\frac{\overline{vt}}{U_{\infty}(T_e - T_s)}$
0.068	+4.89	+0.00596	+7.96	+0.0383
0.118	-2.74	- 0.00405	+1.74	+0.00837
0.168	-3.35	-0.00496	+0.421	+0.00202
0.218	-1.41	-0.00209	+0.633	+0.00304
0.268	-0.641	-0.00095	+0.737	+0.00354
0.368	-0.205	-0.00030	+0.686	+0.00330
0.468	+0.008	+0.00000	+0.693	+0.00333

APPENDIX F

REFERENCES

(1) Johnson, Donald S., Turbulent Heat Transfer in a Boundary Layer with Discontinuous Wall Temperature, OSR TN 55-289, Dept. of Aeronautics, The Johns Hopkins University, August 1955.

(2) Kovasznay, L.S.G., Development of Turbulence-Measuring Equipment, NBS, NACA Report 1209 (formerly TN 2839), July 1953.

(3) Kovasznay, L., Calibration and Measurement in Turbulent Research by the Hot-Wire Method, NACA TM 1130, June 1947.

(4) Cousin, Stanley, Extended Applications of the Hot Wire Anemometer, CIT, NACA TN 1864, April 1949.

(5) Elias, Franz, The Transference of Heat from a Hot Plate to an Airstream, NACA TM 614, 1931.

(6) Weske, J. R., Methods of Measurement of High Air Velocities by the Hot Wire Method, Case School of Applied Science, NACA TN 880, February 1943.

(7) Lowell, Herman H., Design and Applications of Hot-Wire Anemometer for Steady State Measurements at Transonic and Supersonic Air Speeds, NACA TN 2117, July 1950.

(8) Cousin, S. and Kistler, A.L., Free Stream Boundaries of Turbulent Flows, NACA REPORT 1244 (Formerly NACA TN 3133), 1955.

(9) Dosanjh, D. S., Use of a Hot-Wire Anemometer in Shock Tube Investigations, NACA TN 3163, December 1954.

(10) Winovich, W. and Stine, H. A., Measurements of the Nonlinear Variation with Temperature of Heat-Transfer Rate from Hot Wires in Transonic and Supersonic Flow, NACA TN 3965, April 1957.

(11) Spangenberg, W. G., Heat Loss Characteristics of Hot-Wire Anemometers at Various Densities in Transonic and Supersonic Flow, NACA TN 3381, NBS, May 1955.

APPENDIX D

REFERENCES

(1) Johnson, Donald S., Turbulent Heat Transfer in a Boundary Layer with Discontinuous Wall Temperature, ONR TR 55-289, Dept. of Aeronautics, The Johns Hopkins University, August 1955.

(2) Kovasznay, L.S.G., Development of Turbulence-Measuring Equipment, NBS, NACA Report 1209 (formerly TN 2339), July 1953.

(3) Kovasznay, L., Calibration and Measurement of Turbulent Research by the Hot-Wire Method, NACA TM 1130, June 1947.

(4) Cousin, Stanley, Improved Applications of the Hot Wire Anemometer, CIT, NACA TN 1864, April 1949.

(5) Ellis, Frank, The Transference of Heat from a Hot Plate to an Airstream, NACA TN 614, 1931.

(6) Weske, J. R., Methods of Measurement of High Air Velocities by the Hot Wire Method, Case School of Applied Science, NACA TN 690, February 1943.

(7) Lowell, Herman H., Design and Applications of Hot-Wire Anemometer for Steady State Measurements at Transonic and Supersonic Air Speeds, NACA TN 2117, July 1950.

(8) Cousin, S. and Platter, A.L., Free Stream Boundaries of Turbulent Flows, NACA REPORT 1244 (Formerly NACA TN 2133), 1955.

(9) Beranjh, D. R., Use of a Hot-Wire Anemometer in Shock Tube Investigations, NACA TN 3163, December 1954.

(10) Hrycak, W. and Stine, H. A., Measurements of the Nonlinear Variation with Temperature of Heat-Transfer Rate from Hot Wires in Turbulent and Supersonic Flow, NACA TN 3965, April 1957.

(11) Spangenberg, W. G., Some Loss Characteristics of Hot-Wire Anemometers in Viscous Regulated in Transonic and Supersonic Flow, NACA TN 1381, [illegible], May 1955.

(12) Model HWB Hot Wire Anemometer - Theory and Instructions, Flow Corporation, Arlington, Mass.

(13) Selected Topics in Hot-Wire Anemometer Theory, Bulletin No. 25, Flow Corporation, Arlington, Mass.

(14) Braga, L.E.M., Heat Transfer from a Flat Plate with Arbitrary Surface Temperature to a Turbulent Boundary Layer, Master's Thesis, M.I.T., September 1957.

(12) Model NAW Hot Wire Anemometer - Theory and Instructions, Flow Corporation, Arlington, Mass.

(13) Selected Topics in Hot-Wire Anemometer Theory, Bulletin No. 25, Flow Corporation, Arlington, Mass.

(14) Brege, R.A.M., Heat Transfer from a Flat Plate with Arbitrary Surface Temperature to a Turbulent Boundary Layer, Master's Thesis, M.I.T., September 1952.